cleaned of excessive perivascular tissue, and frozen in liquid nitrogen. Total RNA was reverse transcribed, and the resultant cDNA was amplified by TaqMan Real-Time Reverse Transcription-PCR on the ABI Prism 7000 Sequence Detection as described previously.[18] The respective PCR primers and TaqMan probes were designed from GenBank databases using a software program (Applied Biosystems; Table 1). The results were analyzed using the Sequence Detection Software (Applied Biosystems) and expressed in arbitrary units and adjusted for GAPDH mRNA levels.

Measurement of antibody productions in 7ND-transfected animals

We examined whether anti-7ND IgG and IgM antibodies were produced in 7ND-transfected monkeys. In all, 96-well plates (ELISA PLATE HTYPE, SUMITOMO BAKELITE Co., Ltd.) were coated with 7ND protein (0.1 μg/ml). Paired serum before and 7 or 28 days after 7ND transfection was incubated on each coated well for 90 min at 37°C followed by incubation with HRP-conjugated goat antibodies against monkey IgG or IgM (Kirkegaard & Perry Laboratories) for 1–2 h at 37°C. TMB one solution (Promega) was used, and the absorbencies of each well were detected by using ELISA plate reader.

Statistical analysis

Data are expressed as the mean ± s.e. Statistical analysis of differences was compared by analysis of variance and Bonferroni's multiple comparison tests. A *P*-value of less than 0.05 was considered to be statistically significant.

Acknowledgements

This study was supported by Grants-in-Aid for Scientific Research (14657172, 14207036) from the Ministry of Education, Science, and Culture, Tokyo, Japan, by Health Science Research Grants (Comprehensive Research on Aging and Health, and Research on Translational Research) from the Ministry of Health Labor and Welfare, Tokyo, Japan, and by the Program for Promotion of Fundamental Studies in Health Sciences of the Organization for Pharmaceutical Safety and Research, Tokyo, Japan.

References

1 Topol EJ, Serruys PW. Frontiers in interventional cardiology. *Circulation* 1998; **98**: 1802–1820.
2 Hoffmann R *et al*. Patterns and mechanisms of in-stent restenosis. A serial intravascular ultrasound study. *Circulation* 1996; **94**: 1247–1254.
3 Farb A *et al*. Pathology of acute and chronic coronary stenting in humans. *Circulation* 1999; **99**: 44–52.
4 Grewe PH *et al*. Acute and chronic tissue response to coronary stent implantation: pathologic findings in human specimen. *J Am Coll Cardiol* 2000; **35**: 157–163.
5 Kornowski R *et al*. In-stent restenosis: contributions of inflammatory responses and arterial injury to neointimal hyperplasia. *J Am Coll Cardiol* 1998; **31**: 224–230.
6 Suzuki T *et al*. Stent-based delivery of sirolimus reduces neointimal formation in a porcine coronary model. *Circulation* 2001; **104**: 1188–1193.
7 Sousa JE *et al*. Sustained suppression of neointimal proliferation by sirolimus-eluting stents: one-year angiographic and intravascular ultrasound follow-up. *Circulation* 2001; **104**: 2007–2011.
8 Teirstein PS. Living the dream of no restenosis. *Circulation* 2001; **104**: 1996–1998.
9 Morice MC *et al*. A randomized comparison of a sirolimus-eluting stent with a standard stent for coronary revascularization. *N Engl J Med* 2002; **346**: 1773–1780.
10 Farb A *et al*. Morphological predictors of restenosis after coronary stenting in humans. *Circulation* 2002; **105**: 2974–2980.
11 Sousa JE, Costa MA, Sousa AG. What is 'the matter' with restenosis in 2002? *Circulation* 2002; **105**: 2932–2933.
12 Welt FG, Rogers C. Inflammation and restenosis in the stent era. *Arterioscler Thromb Vasc Biol* 2002; **22**: 1769–1776.
13 Gerard C, Rollins BJ. Chemokines and disease. *Nat Immunol* 2001; **2**: 108–115.
14 Mukaida N, Harada A, Matsushima K. Interleukin-8 (IL-8) and monocyte chemotactic and activating factor (MCAF/MCP-1), chemokines essentially involved in inflammatory and immune reactions. *Cytokine Growth Factor Rev* 1998; **9**: 9–23.
15 Egashira K *et al*. Anti-monocyte chemoattractant protein-1 gene therapy inhibits vascular remodeling in rats: blockade of MCP-1 activity after intramuscular transfer of a mutant gene inhibits vascular remodeling induced by chronic blockade of NO synthesis. *FASEB J* 2000; **14**: 1974–1978.
16 Zhang Y, Rollins BJ. A dominant negative inhibitor indicates that monocyte chemoattractant protein 1 functions as a dimer. *Mol Cell Biol* 1995; **15**: 4851–4855.
17 Egashira K *et al*. Importance of monocyte chemoattractant protein-1 pathway in neointimal hyperplasia after periarterial injury in mice and monkeys. *Circ Res* 2002; **90**: 1167–1172.
18 Usui M *et al*. Anti-monocyte chemoattractant protein-1 gene therapy inhibits restenotic changes (neointimal hyperplasia) after balloon injury in rats and monkeys. *FASEB J* 2002; **16**: 1838–1840.
19 Mori E *et al*. Essential role of monocyte chemoattractant protein-1 in development of restenotic changes (neointimal hyperplasia and constrictive remodeling) after balloon angioplasty in hypercholesterolemic rabbits. *Circulation* 2002; **105**: 2905–2910.
20 Ni W *et al*. New anti-monocyte chemoattractant protein-1 gene therapy attenuates atherosclerosis in apolipoprotein E-knockout mice. *Circulation* 2001; **103**: 2096–2101.
21 Inoue S *et al*. Anti-monocyte chemoattractant protein-1 gene therapy limits progression and destabilization of established atherosclerosis in apolipoprotein E-knockout mice. *Circulation* 2002; **106**: 2700–2706.
22 Roque M *et al*. CCR2 deficiency decreases intimal hyperplasia after arterial injury. *Arterioscler Thromb Vasc Biol* 2002; **22**: 554–559.
23 Horvath C *et al*. Targeting CCR2 or CD18 inhibits experimental in-stent restenosis in primates: inhibitory potential depends on type of injury and leukocytes targeted. *Circ Res* 2002; **90**: 488–494.
24 Schwartz RS *et al*. Drug-eluting stents in preclinical studies: recommended evaluation from a consensus group. *Circulation* 2002; **106**: 1867–1873.
25 Rogers C, Edelman ER. Endovascular stent design dictates experimental restenosis and thrombosis. *Circulation* 1995; **91**: 2995–3001.
26 Rogers C, Edelman ER, Simon DI. A mAb to the beta2-leukocyte integrin Mac-1 (CD11b/CD18) reduces intimal thickening after angioplasty or stent implantation in rabbits. *Proc Natl Acad Sci USA* 1998; **95**: 10134–10139.
27 Cipollone F *et al*. Elevated circulating levels of monocyte chemoattractant protein-1 in patients with restenosis after

coronary angioplasty. *Arterioscler Thromb Vasc Biol* 2001; **21**: 327–334.
28 Oshima S *et al*. Plasma monocyte chemoattractant protein-1 antigen levels and the risk of restenosis after coronary stent implantation. *Jpn Circ J* 2001; **65**: 261–264.
29 Farb A *et al*. Oral everolimus inhibits in-stent neointimal growth. *Circulation* 2002; **106**: 2379–2384.
30 Inadera H *et al*. Increase in circulating levels of monocyte chemoattractant protein-1 with aging. *J Interferon Cytokine Res* 1999; **19**: 1179–1182.
31 de Lemos JA *et al*. Association between plasma levels of monocyte chemoattractant protein-1 and long-term clinical outcomes in patients with acute coronary syndromes. *Circulation* 2003; **107**: 690–695.

Cholesterol-Lowering Independent Regression and Stabilization of Atherosclerotic Lesions by Pravastatin and by Antimonocyte Chemoattractant Protein-1 Therapy in Nonhuman Primates

Shiro Kitamoto, Kaku Nakano, Yasuhiko Hirouchi, Yoshiro Kohjimoto, Shunichi Kitajima, Makoto Usui, Shujiro Inoue, Kensuke Egashira

Objective—Anti-atherosclerotic effects of statins might be mediated partly by pleiotropic cholesterol-lowering independent mechanisms. We used nonhuman primates and examined whether treatment with pravastatin or antimonocyte chemoattractant protein-1 (MCP-1) therapy can induce regression and stabilization of established atherosclerotic lesions through cholesterol-lowering independent mechanisms.

Methods and Results—Advanced atherosclerosis was induced in the abdominal aorta and the common iliac artery of cynomolgus monkeys by undergoing balloon injury and giving atherogenic diet for 6 months. At 6 months, the diet was changed to normal chow, and the animals were allocated to 4 treatment groups: control vehicle group and other groups treated with pravastatin (1 or 10 mg/kg) or with mutant MCP-1 gene transfection for additional 6 months. Each compound was treated instead of the atherogenic diet, and cholesterol contents in pravastatin-treated groups were adjusted to equalize plasma cholesterol level among groups. Pravastatin reduced neointimal formation in the aorta, but not in the common iliac artery. Pravastatin reduced intimal macrophage area and other markers of plaque destabilization in the common iliac artery. Equivalent inhibitory effects were observed in animals that received mutant MCP-1 gene transfection. No serious side effects were noted by 2 therapeutic modalities.

Conclusion—This study demonstrated cholesterol-lowering independent regression and stabilization of established atherosclerotic lesions by pravastatin and by anti-MCP-1 therapy in nonhuman primates. An anti-inflammatory mechanism may be involved in the beneficial effects of pravastatin. (***Arterioscler Thromb Vasc Biol.* 2004; 24:1522-1528.**)

Key Words: atherosclerosis ■ 3-hydroxy-3-methylglutaryl-coenzyme A reductase inhibitors ■ nonhuman primates ■ inflammation ■ regression

There is clinical evidence that 3-hydroxyl-3-methylglutaryl-coenzyme A reductase inhibitors (statins) improve endothelial dysfunction and reduce the incidence of atherosclerotic events such as myocardial infarctions and ischemic strokes.[1–4] Although anti-atherosclerotic effects of statins are attributed to their lipid-lowering effects, it is suggested that some of the beneficial effects of statins are mediated by pleiotropic effects independent of cholesterol-lowering.[1–3,5–7] There is ample evidence that statins improve endothelial dysfunction[8,9] and reduce vascular inflammation and oxidative stress[10] by their cholesterol-lowering independent effects. These data suggest the possibility that treatment with statins has cholesterol-lowering independent anti-atherosclerotic effects in humans. It is practically impossible, however, to investigate such beneficial effects of statins in clinical settings, because clinical doses of statins inevitably lower serum cholesterol levels.

Nonhuman primate models may be useful to gain insight into cholesterol-lowering independent anti-atherosclerotic effects of statins. There are at least 2 studies that had examined cholesterol-lowering independent effects of statins on atherosclerosis in cynomolgus monkeys. Sukhova et al[11] reported that statins reduced markers of plaque destabilization, and Williams et al[12] reported that pravastatin improved endothelial dysfunction and reduced macrophage infiltration of coronary arteries. These studies, however, failed to demonstrate reduction or regression of atherosclerosis formation by statins. One notable caveat in interpreting these previous studies is that a high dose (20 or 40 mg/kg per day) of pravastatins was used, which might cause serious side effects.

Received April 5, 2004; revision accepted May 20, 2004.

From the Department of Cardiovascular Medicine (S.K., K.N., M.U., S.I., K.E.), Graduate School of Medical Sciences, Kyushu University, Fukuoka, Japan; and Primate LTD (H.Y., Y.K., S.K.), Kumamoto, Japan.

Correspondence to Dr Kensuke Egashira, Department of Cardiovascular Medicine, Graduate School of Medical Sciences, Kyushu University, 3-1-1, Maidashi, Higashi-ku, Fukuoka 812-8582, Japan. E-mail egashira@cardiol.med.kyushu-u.ac.jp

Arterioscler Thromb Vasc Biol. **is available at http://www.atvbaha.org** **DOI: 10.1161/01.ATV.0000134518.27241.da**

In the present study, we aimed to investigate cholesterol-lowering independent effects of pravastatin on regression and stabilization of established atherosclerotic lesions in nonhuman primates (cynomolgus monkeys). For clinical implication, we selected at least a clinical dose of pravastatin (1 mg/kg per day). To obtain mechanistic data regarding anti-inflammatory effects, we examined whether anti-atherosclerotic actions afforded by pravastatin resemble those obtained by antimonocyte chemoattractant protein-1 (MCP-1) therapy. Because recruitment of monocyte/macrophage is a major histopathologic finding in atherosclerosis, an anti-inflammatory strategy targeting MCP-1 is considered to be a reasonable approach for vascular inflammation leading to atherosclerosis.[13] We have recently devised a new strategy of anti-MCP-1 gene therapy by transfecting plasmid cDNA encoding a mutant MCP-1 gene into skeletal muscle.[14] This mutant MCP-1, called 7ND, lacks the N-terminal amino acid 2 to 8 and has been shown to work as a dominant-negative inhibitor of MCP-1. With this strategy, we have demonstrated that blockade of MCP-1 signals reduces neointimal formation after arterial injury in animals, including monkeys.[15–17] We report here that treatment with pravastatin or anti-MCP-1 therapy not only reduced plaque size but also changed characteristics of plaques to more stable phenotype in cynomolgus monkeys with established atherosclerotic lesion caused by arterial injury and hypercholesterolemia.

Methods

Experimental Animals

Forty-five 4-year-old male cynomolgus monkeys were used. The study protocol was reviewed and approved by the Committee on the Ethics of Animal Experiments, Kyushu University Graduate School of Medical Sciences. A part of this study was performed at the Station for Collaborative Research and the Morphology Core, Kyushu University Graduate School of Medical Sciences.

Treatment and Tissue Preparation

All animals were fed a high-cholesterol diet (0.5% cholesterol and 6% corn oil) for 6 months and received balloon injury of the descending aorta and the right common iliac artery at 1 month after the initiation of the diet. Nine animals were euthanized after 6 months of high-cholesterol diet and were considered the baseline group. Thereafter, the diet was changed to normal chow, and the animals were randomized to 4 groups as follows: (1) vehicle control group (0.5% carboxymethyl cellulose sodium salt); (2) low-dose pravastatin (1 mg/kg per day) group (low-P group); (3) high-dose pravastatin (10 mg/kg per day) group (high-P group); and (4) 7ND transfection group (n=9 each). In the animals treated with pravastatin, 0.4% to 4% cholesterol solution was orally administered and adjusted on a biweekly basis to make the serum cholesterol level equal to that in the vehicle group.

To transfect 7ND gene, 7ND plasmid (2.5 mg/500 μL PBS) was injected into the femoral muscle of the animals in the 7ND group biweekly. To enhance transgene expression, all monkeys were pretreated with intramuscular injection of bipuvacine (0.25 mg/kg) at the injected site.[18] Human 7ND cDNA was constructed by recombinant polymerase chain reaction using a wild-type human MCP-1 cDNA as template and inserted into the *Bam*HI (5′) and *Not*I (3′) sites of the pcDNA3 (Invitrogen) expression vector plasmid.[14] We have reported biological efficacy of 7ND gene transfer by in vivo matrigel plug assay in monkeys.[18] In brief, MCP-1-induced inflammatory angiogenesis in the plugs was suppressed until 14 days after 7ND gene transfer. All monkeys were euthanized with a lethal dose of anesthesia after 6 months of treatment for morphometric analysis (Figure 1A).

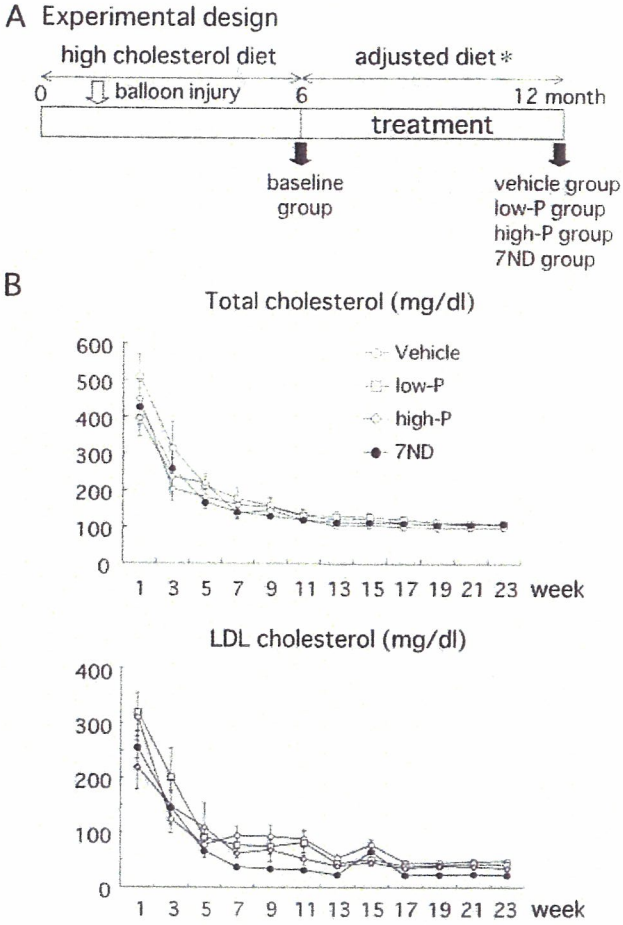

Figure 1. Experimental design and serum cholesterol levels. A, Experimental design. B, Time courses of serum cholesterol levels in the 4 treatment groups. *0.4% to 4% cholesterol solution was orally administered in pravastatin-treated groups to equalize plasma cholesterol level among 4 groups.

After the monkeys were euthanized, the abdominal aortas and the right iliac arteries were perfused with saline and fixed with the solution of 95% ethanol and 1% acetic acid and were used for histology and immunohistochemistry.

Histology and Immunohistochemistry

All tissues were dehydrated and embedded in paraffin, and serial sections (5 μm) of the abdominal aortas and the common iliac arteries were prepared and mounted on slides. Some of these sections were stained with hematoxylin-eosin, Elastica van Gieson, or Elastica Masson. Interstitial collagens were stained by Picrosirius red (Direct Red, Aldrich Chem) and photographed using a polarization microscopy. The remaining sections were used for immunohistochemical analysis. They were stained with an antibody for smooth muscle cell (mouse anti-human HHF-35 antibody, DAKO, Kyoto, Japan), macrophages/monocytes (mouse anti-human CD-68 antibody, DAKO), or nonimmune mouse IgG (DAKO). After incubation with appropriate biotinylated affinity-purified secondary antibodies (DAKO), the sections were incubated with alkaline phosphatase-labeled streptavidin solution (DAKO) and visualized using a fast red substrate kit (DAKO). The sections were then counterstained with Karachi-hematoxylin.

A single observer who was blinded to the experiment protocol performed morphometry and cell counting. All images were captured by an Olympus microscope equipped with a digital camera (HC-2500) and were analyzed using Adobe Photoshop 6.0 and National

TABLE 1. Body Weight and Biochemical Parameters in Experimental Groups

Groups	Baseline (n=9)	Vehicle (n=9)	Low-P (n=9)	High-P (n=9)	7ND (n=9)
Parameters					
Body weight	5.13±0.11	5.73±0.30	5.52±0.29	5.07±0.23	5.07±0.23
Total cholesterol (mg/dl)	473±41	110±6**	118±9**	103±7**	125±9**
LDL cholesterol (mg/dl)	436±37	43±3**	47±4**	47±4**	53±4**
Triglyceride (mg/dl)	9±1	23±3**	21±2**	25±2**	21±2**
AST (U/L)	48±7	30±1**	28±2**	29±2**	39±10*
ALT (U/L)	10±2	38±3**	36±3**	38±4**	39±4**
CPK (U/L)	645±176	188±40**	150±14**	135±20**	144±12*
Glucose (mg/dl)	60±2	59±2	61±2	58±2	60±2

Data are mean±SE. *$P<0.05$, **$P<0.01$ versus baseline group.

LDL indicates low density lipoprotein; AST, aspartate aminotransferase; ALT, alanine aminotransferase; CPK, creatine phosphokinase.

Institute of Health Image 1.62 Software. Elastica-van Gieson staining, which stains elastic fiber, was used to delineate internal elastic lamina for determination of the intimal area. The percent area of extracellular lipid deposition (area dropped off in Elastica Masson staining), macrophage accumulation (CD68-positive area), smooth muscle cell area (HHF-35–positive area), and collagen deposition (Picrosirius red staining area) were estimated.

Biochemical Analysis and Measurements of Cytokines

Biochemical parameters listed in Tables 1 and 2 were measured by SRL Inc, Japan. Chemokines including MCP-1, IL-8, and transforming growth factor-β1 (TGF-β1) were measured using commercially available enzyme-linked immunosorbent assay (ELISA) kits (Biosource International Inc).

Measurement of Antibody Productions in 7ND-Transfected Animals

We examined whether anti-7ND or anti-MCP-1 IgG and IgM antibodies were produced in the 7ND transfected animals. Ninety-six well plates were coated with 7ND protein (0.1 μg/mL) or with human MCP-1 protein (0.1 μg/mL). Paired serum before and 7 or 28 days after 7ND transfection was incubated on each coated well for 90 minutes at 37°C, followed by incubation with HRP-conjugated goat antibodies against monkey IgG or IgM (Kirkegaard & Perry Laboratories) for 1 to 2 hours at 37°C. TMB one solution (Promega) was used, and the absorbencies of each well were detected by using an ELISA plate reader.

We also checked the presence of newly produced immunoglobulins in the 7ND-transfected animals 11 and 17 months after transfection. The control monkey serum and the 7ND-treated monkey serum were diluted 500-fold, and the diluted serum was mixed with an equivalent solution of 4% SDS in Tris buffer, and the solution was boiled for 5 minutes. The treated protein solution was then electrophoresed on a 5% to 20% polyacrylamide gradient gel according to the method of Laemmli. The developed protein bands on the gel were visualized by staining with SYPRO Ruby. Molecular weight was determined in comparison with the molecular weight markers.

Statistical Analysis

Data were expressed as mean±SEM. Differences between groups were determined using 2-way analysis of variance and a multiple comparison test. $P<0.05$ was considered to be statistically significant.

Results

Clinical Status and Biochemical Parameters

All animals had no clinical signs (decreased spontaneous motor action, decreased food consumption, diarrhea, limping, and prone position) during experimental period and survived. There was no significant treatment effect on body weight among 4 groups (Table 1). Pravastatin treatment and 7ND gene transfection had no adverse effects on biochemical parameters, including CPK and liver transaminases (Table 1). As designed, time courses of serum total cholesterol levels and low-density lipoprotein cholesterol levels were comparable among 4 groups (Figure 1B, $P>0.10$).

There were also no treatment effects on plasma renin activity or angiotensin II in the pravastatin groups and 7ND group (Table 2). Plasma MCP-1 levels in all groups decreased with time. However, pravastatin treatment and 7ND gene transfection had no treatment effect on cytokine concentrations (Table 2).

Pravastatin-Induced Regression of Atherosclerotic Lesions in Abdominal Aorta

There was no significant difference in the degrees of neointimal formation (intimal area and intima/media ratio) between the baseline group and the vehicle group. In contrast, pravastatin treatment and 7ND gene transfer significantly reduced neointimal formation of injured abdominal aorta compared with the vehicle group (Figure 2, Table 3). There was no difference in medial area among 4 treatment groups.

Pravastatin Changes Characteristics of Atheromatous Plaques Composition

In common iliac arteries, although significant reduction of intimal area was noted in the 7ND group, there were no treatment effects on the intima/media ratio in the pravastatin group and the 7ND group compared with the vehicle group (Figure 3, Table 3).

Because neither pravastatin nor 7ND reduced the neointimal formation in the common iliac arteries, we then investigated the characteristics of plaque composition (Figure 4). Macrophage infiltration into atherosclerotic lesion was markedly less in the pravastatin groups and the 7ND group compared with the vehicle group. Percent areas of lipid deposition were also reduced in the pravastatin groups and the 7ND group compared with the vehicle

TABLE 2. Time Course of Angiotensin Converting Enzyme Activity, Plasma Renin Activity, and Plasma Concentrations of Angiotensin II and Inflammatory Cytokines in Experimental Groups

			Weeks After Initiation of Treatment		
	Groups	Baseline	1	12	24
ACE (U/L)	baseline	55±4	—	—	—
	vehicle	—	42±3	52±4	52±5
	low-P	—	48±4	56±5	60±5
	high-P	—	44±3	48±4	53±5
	7ND	—	50±4	58±5	59±5
Renin (ng/mL/hr)	baseline	8±4	—	—	—
	vehicle	—	9±1	8±1	8±2
	low-P	—	8±1	10±2	7±2
	high-P	—	6±1	15±5	7±1
	7ND	—	5±1	8±1	8±4
Angiotensin II (pg/mL)	baseline	12±5	—	—	—
	vehicle	—	11±1	13±1	41±6
	low-P	—	7±2	12±2	34±7
	high-P	—	9±2	17±2	40±7
	7ND	—	8±2	16±4	29±8
MCP-1 (pg/mL)	baseline	262±49	—	—	—
	vehicle	—	605±142	229±20	190±30
	low-P	—	441±111	212±24	194±26
	high-P	—	302±54	247±45	204±24
	7ND	—	329±82	214±18	193±29
IL-8 (pg/mL)	baseline	105±17	—	—	—
	vehicle	—	155±23	284±29	180±26
	low-P	—	152±18	247±33	170±40
	high-P	—	139±19	236±42	259±56
	7ND	—	185±16	197±36	276±63
TGF-β1 (ng/mL)	baseline	47±6	—	—	—
	vehicle	—	59±6	49±3	60±4
	low-P	—	53±8	44±4	51±4
	high-P	—	49±6	50±9	50±7
	7ND	—	49±4	62±6	64±4

Data are mean±SE.

ACE indicates angiotensin converting enzyme; MCP-1, monocyte chemoattractant protein-1; IL-8, interleukin-8; TGF-β1, transforming growth factor-β1.

group. However, there was no significant difference in the percent area of collagen and smooth muscle cells among 4 treatment groups.

Antibody Production in 7ND-Transfected Animals

In ELISA assay, IgG and IgM antibodies against 7ND protein and wild-type MCP-1 protein were not detected after 7ND transfection (n=6 each). The electrophoresis pattern of the7ND-transfected monkey serum was almost consistent with that of the control monkey serum, and the abnormal bands of immunoglobulin heavy chain protein and light chain protein were not observed in the electrophoresis result of the 7ND-transfected monkey serum compared with that of the control monkey serum (Figure 5).

Discussion

A novel finding of this study was that compared with dietary lipid-lowering therapy alone, additional treatment with pravastatin induced regression of established atherosclerotic lesions of the injured abdominal aorta in nonhuman primates. In contrast, pravastatin did not reduce the size but induced stabilization of atherosclerotic lesions of the common iliac arteries, suggesting that the effects of the statin on regression might differ according to the size/site of artery. Because of our experimental design, these beneficial effects on regression and stabilization were independent of the cholesterol-lowering effects of the statin. Overall, the present data provide the notion that pravastatin treatment in addition to strong dietary lipid-lowering can induce regression and

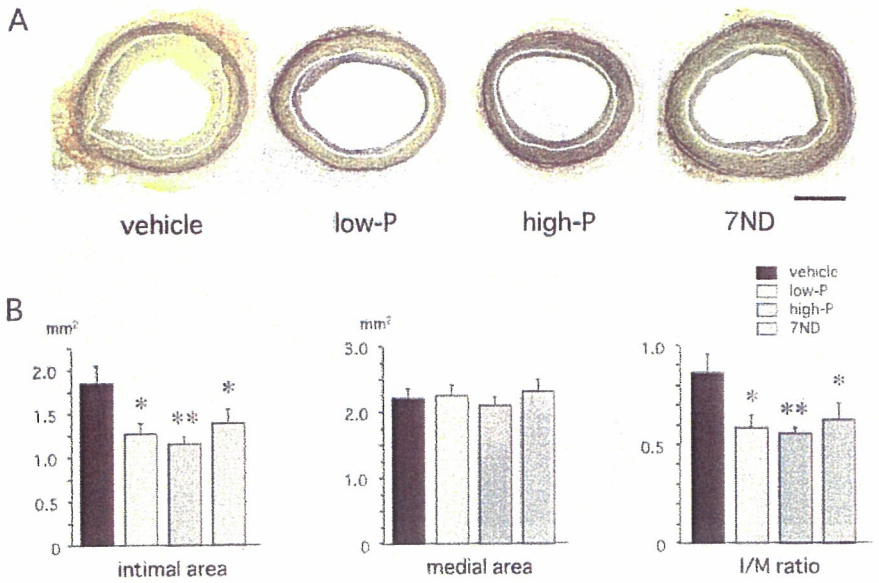

Figure 2. Effects of pravastatin or 7ND transfection on atherosclerosis in the abdominal aorta. A, Representative photomicrographs of cross-sections of the injured abdominal aortas stained with Elastica van Gieson in 4 treatment groups. Internal elastic laminae are outlined with white. B, Intimal area, medial area, and intima/media (I/M) ratio of the injured abdominal aortas. *$P<0.05$, **$P<0.01$ versus vehicle group.

plaque stabilization of atherosclerotic lesions by mechanisms beyond its cholesterol-lowering effects.

Previous studies in animals have not addressed cholesterol independent regression of atherosclerosis by statins. As mentioned, 2 recent studies that examined effects of statins on atherogenesis in cynomolgus monkeys[11,12] showed no detectable reduction in plaque size after statin treatment. Our model differs from those models in several aspects that deserve discussion. First, in addition to high-cholesterol diet, balloon injury was performed in the present study. Balloon injury to hypercholesterolemic animals accelerates atheroma formation and makes lesions more uniform in size.[19,20] Importantly such injured lesions resemble the so-called vulnerable plaque in humans more closely, compared with the foam cells and macrophage-rich lesions produced by hypercholesterolemia alone. Therefore, it is possible that such "vulnerable" plaque was more sensitive to pravastatin treatment. Second, we used relatively lower doses of pravastatin (1 mg/kg and 10 mg/kg per day) compared with the previous studies (20 mg/kg or 40 mg/kg per day). The low dose (1 mg/kg per day) used in the present study is the range of clinical doses. Therefore, the present data imply that a clinically relevant dose of pravastatin can induce regression and stabilization of atherosclerotic lesions in nonhuman primates. Reasons why the higher doses (10 mg/kg per day or more) of pravastatin could not show greater action on regression and stabilization of atherosclerosis in our present study and previous studies are not clear. In preliminary experiments, we administered higher doses (20 and 30 mg/kg per day) of pravastatin to hypercholesterolemic monkeys, which resulted in serious side effects such as body weight loss and labdomyolysis leading to death (data not shown). We speculate, therefore, that some toxic actions at high doses of pravastatin might detract from beneficial effects of the low dose of pravastatin in the present and those previous studies.

It has been shown that increased macrophage infiltration and lipid deposition enhance plaque destabilization and that increased interstitial collagens and smooth muscle cells increase plaque stability.[21] We show here that pravastatin did not affect percent areas of collagen and smooth muscle cells but did reduce the degrees of macrophage infiltration and lipid deposition into atherosclerotic plaque of the common iliac arteries. These data support the previous reports that treatment with statins promotes transformation of destabilized plaque of atheroma to more stable phenotype through cholesterol-lowering independent actions.

TABLE 3. Histological Analysis of the Abdominal Aortas and the Common Iliac Arteries in Experimental Groups

Groups	Baseline (n=9)	Vehicle (n=9)	Low-P (n=9)	High-P (n=9)	7ND (n=9)
Abdominal aorta					
Intimal area (mm²)	1.5±0.2	1.8±0.2	1.3±0.1*	1.2±0.1**	1.4±0.2*
Medial area (mm²)	1.9±0.1	2.2±0.2	2.2±0.2	2.1±0.1	2.3±0.2
I/M ratio	0.8±0.1	0.9±0.1	0.6±0.1*	0.6±0.0**	0.6±0.1*
Common iliac artery					
Intimal area (mm²)	0.8±0.1	1.3±0.2	0.9±0.2	0.9±0.2	0.8±0.1*
Medial area (mm²)	1.0±0.0	1.1±0.1	0.9±0.1	0.9±0.1	1.0±0.1
I/M ratio	0.8±0.1	1.5±0.4	1.1±0.2	1.3±0.4	0.8±0.2

Data are mean±SE.
*$P<0.05$, **$P<0.01$ versus vehicle group.

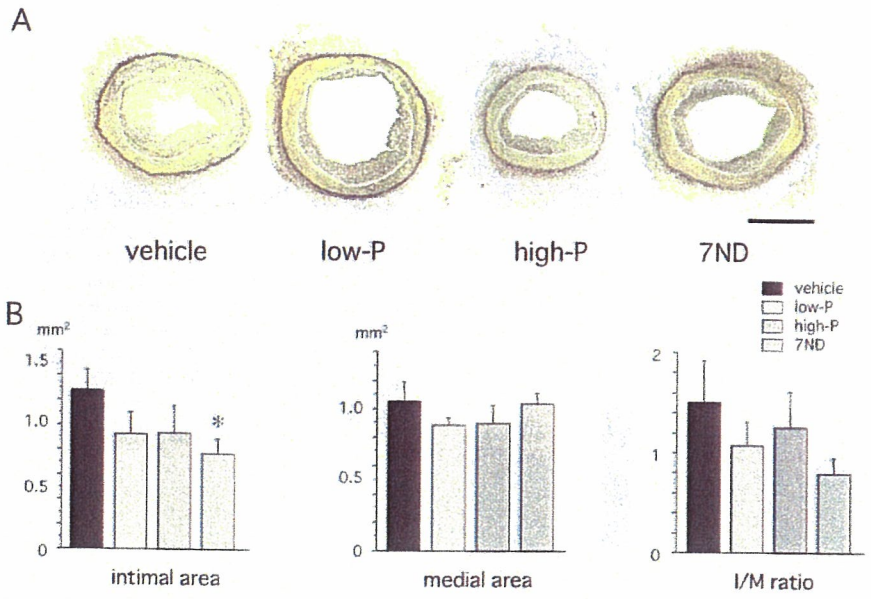

Figure 3. Effects of pravastatin or 7ND transfection on atherosclerosis in the common iliac artery. A, Representative photomicrographs of cross-sections of the injured common iliac arteries stained with Elastica van Gieson in 4 treatment groups. Internal elastic laminae are outlined with white. B, Intimal area, medial area, and intima/media (I/M) ratio of the injured iliac arteries. * $P<0.05$, ** $P<0.01$ versus vehicle group.

We[13,15,17,18,22,23] have previously shown that blockade of MCP-1 by 7ND gene transfer reduces neointimal formation after mechanical injury and initiation and progression of hypercholesterolemia-induced atherosclerosis by suppressing monocyte infiltration and activation. We therefore examined whether the observed effects of pravastatin were similar to those of 7ND gene transfer and found that the effects of pravastatin on plaque size and composition were comparable to those obtained by 7ND gene transfer. Of note is that striking decreases in macrophage infiltration and lipid deposition were achieved by pravastatin treatment and by 7ND gene transfer. Reduced local lipid deposition might be the result of reduced macrophage infiltration. These data imply that pravastatin might function as local anti-inflammatory or anti-MCP-1 therapy beyond its cholesterol-lowering effects. We further examined whether systemic inflammatory process was involved and showed that there were no treatment effects of pravastatin or 7ND gene transfer on plasma concentrations of chemokines and cytokines listed in Table 2. These data suggest that the observed beneficial effects of pravastatin in the present study may not be mediated by its inhibitory effects on plasma MCP-1, renin-angiotensin system, and other systemic factors.

No appreciable side effects were observed in animals treated with pravastatin or those that received 7ND gene transfer. Thus, 7ND gene transfer may be as safe as pravastatin, although caution should be used when 7ND is used clinically. 7ND gene transfer can be used clinically because the anti-MCP-1 gene therapy for patients with severe forms of atherosclerotic vascular disease and inflammatory disease cannot be treated successfully by conventional therapeutic regimens.

In conclusion, this study demonstrates that compared with strong dietary lipid lowering alone, additional treatment with pravastatin induces regression and stabilization of established atherosclerotic lesions in nonhuman primates through mechanisms beyond its cholesterol-lowering actions. The observed effects of pravastatin were identical to those of anti-MCP-1 therapy. Thus, an anti-inflammatory mechanism may be involved in the beneficial effects of pravastatin. This study implies that compared with modest to moderate lipid-lowering therapy with statins that have been conventionally introduced to patients with hypercholesterolemia, stronger dietary lipid lowering plus statin treatment may induce significant regression and destabilization of human atherosclerotic lesions resulting in stronger reduction in atherothrombotic events in the patient.

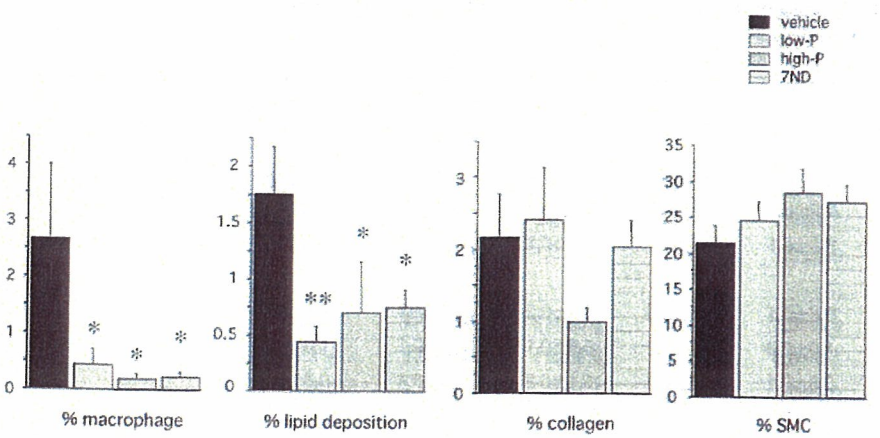

Figure 4. Effects of pravastatin or 7ND transfection on plaque compositions of atherosclerotic lesions of the common iliac artery. *$P<0.05$, **$P<0.01$ versus vehicle group.

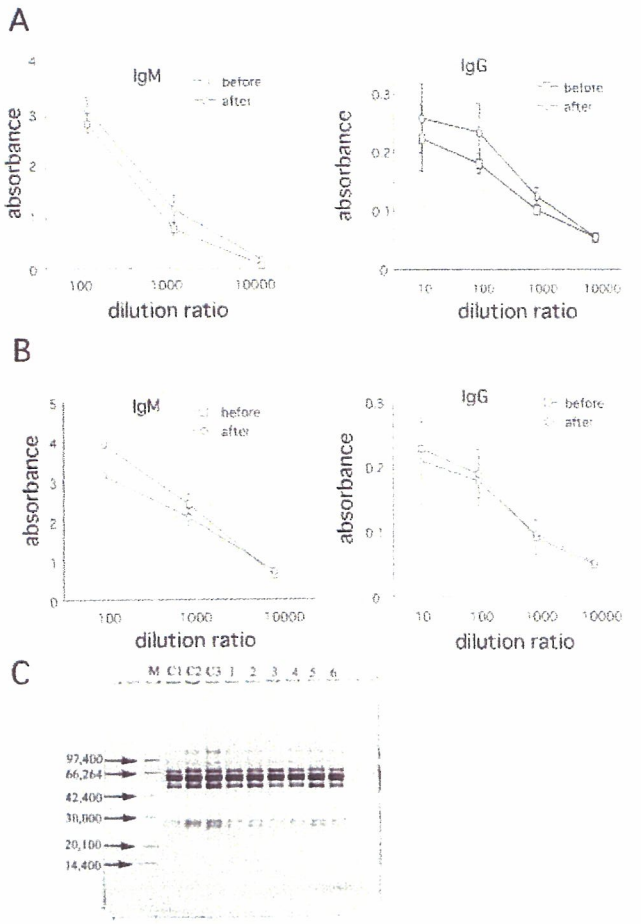

Figure 5. Antibody production in 7ND-transfected animals. A, ELISA assay of anti-7ND antibody (IgM and IgG) in paired serum from 7ND-transfected monkeys. B, ELISA assay of anti-MCP-1 antibody (IgM and IgG) in paired serum from 7ND-transfected monkeys. C, The electrophoresis result of monkey serum. M indicates marker; C1–3, serum from untreated monkeys; 1 to 3, serum from monkeys 11 months after 7ND transfection; 4 to 6, serum from monkeys 17 months after 7ND transfection.

Acknowledgments

This study was supported by grants-in-aid for Scientific Research (14657172, 14207036) from the Ministry of Education, Culture, Sports, Science, and Technology, Tokyo, Japan, by Health Science Research Grants (Comprehensive Research on Aging and Health, and Research on Translational Research) from the Ministry of Health Labor and Welfare, Tokyo, Japan, and by the Program for Promotion of Fundamental Studies in Health Sciences of the Organization for Pharmaceutical Safety and Research, Tokyo, Japan.

References

1. Shepherd J, Cobbe SM, Ford I, Isles CG, Lorimer AR, MacFarlane PW, McKillop JH, Packard CJ. Prevention of coronary heart disease with pravastatin in men with hypercholesterolemia. West of Scotland Coronary Prevention Study Group. *N Engl J Med.* 1995;333:1301–1307.
2. Sacks FM, Pfeffer MA, Moye LA, Rouleau JL, Rutherford JD, Cole TG, Brown L, Warnica JW, Arnold JM, Wun CC, Davis BR, Braunwald E. The effect of pravastatin on coronary events after myocardial infarction in patients with average cholesterol levels. Cholesterol and Recurrent Events Trial investigators. *N Engl J Med.* 1996;335:1001–1009.
3. Randomised trial of cholesterol lowering in 4444 patients with coronary heart disease: the Scandinavian Simvastatin Survival Study (4S). *Lancet.* 1994;344:1383–1389.
4. Egashira K, Hirooka Y, Kai H, Sugimachi M, Suzuki S, Inou T, Takeshita A. Reduction in serum cholesterol with pravastatin improves endothelium-dependent coronary vasomotion in patients with hypercholesterolemia. *Circulation.* 1994;89:2519–2524.
5. Prevention of cardiovascular events and death with pravastatin in patients with coronary heart disease and a broad range of initial cholesterol levels. The Long-Term Intervention with Pravastatin in Ischaemic Disease (LIPID) Study Group. *N Engl J Med.* 1998;339:1349–1357.
6. Influence of pravastatin and plasma lipids on clinical events in the West of Scotland Coronary Prevention Study (WOSCOPS). *Circulation.* 1998; 97:1440–1445.
7. Baseline serum cholesterol and treatment effect in the Scandinavian Simvastatin Survival Study (4S). *Lancet.* 1995;345:1274–1275.
8. Tsunekawa T, Hayashi T, Kano H, Sumi D, Matsui-Hirai H, Thakur NK, Egashira K, Iguchi A. Cerivastatin, a hydroxymethylglutaryl coenzyme a reductase inhibitor, improves endothelial function in elderly diabetic patients within 3 days. *Circulation.* 2001;104:376–379.
9. Masumoto A, Hirooka Y, Hironaga K, Eshima K, Setoguchi S, Egashira K, Takeshita A. Effect of pravastatin on endothelial function in patients with coronary artery disease (cholesterol-independent effect of pravastatin). *Am J Cardiol.* 2001;88:1291–1294.
10. Ni W, Egashira K, Kataoka C, Kitamoto S, Koyanagi M, Inoue S, Takeshita A. Antiinflammatory and antiarteriosclerotic actions of HMG-CoA reductase inhibitors in a rat model of chronic inhibition of nitric oxide synthesis. *Circ Res.* 2001;89:415–421.
11. Sukhova GK, Williams JK, Libby P. Statins reduce inflammation in atheroma of nonhuman primates independent of effects on serum cholesterol. *Arterioscler Thromb Vasc Biol.* 2002;22:1452–1458.
12. Williams JK, Sukhova GK, Herrington DM, Libby P. Pravastatin has cholesterol-lowering independent effects on the artery wall of atherosclerotic monkeys. *J Am Coll Cardiol.* 1998;31:684–691.
13. Egashira K. Molecular mechanisms mediating inflammation in vascular disease: special reference to monocyte chemoattractant protein-1. *Hypertension.* 2003;41:834–841.
14. Egashira K, Koyanagi M, Kitamoto S, Ni W, Kataoka C, Morishita R, Kaneda Y, Akiyama C, Nishida K, Sueishi K, Takeshita A. Anti-monocyte chemoattractant protein-1 gene therapy inhibits vascular remodeling in rats: blockade of MCP-1 activity after intramuscular transfer of a mutant gene inhibits vascular remodeling induced by chronic blockade of NO systhesis. *FASEB J.* 2000;14:1974–1978.
15. Mori E, Komori K, Yamaoka T, Tanii M, Kataoka C, Takeshita A, Usui M, Egashira K, Sugimachi K. Essential role of monocyte chemoattractant protein-1 in development of restenotic changes (neointimal hyperplasia and constrictive remodeling) after balloon angioplasty in hypercholesterolemic rabbits. *Circulation.* 2002;105:2905–2910.
16. Egashira K, Zhao Q, Kataoka C, Ohtani K, Usui M, Charo IF, Nishida K, Inoue S, Katoh M, Ichiki T, Takeshita A. Importance of monocyte chemoattractant protein-1 pathway in neointimal hyperplasia after periarterial injury in mice and monkeys. *Circ Res.* 2002;90:1167–1172.
17. Usui M, Egashira K, Ohtani K, Kataoka C, Ishibashi M, Hiasa K, Katoh M, Zhao Q, Kitamoto S, Takeshita A. Anti-monocyte chemoattractant protein-1 gene therapy inhibits restenotic changes (neointimal hyperplasia) after balloon injury in rats and monkeys. *FASEB J.* 2002;16: 1838–1840.
18. Egashira K. Clinical importance of endothelial function in arteriosclerosis and ischemic heart disease. *Circ J.* 2002;66:529–533.
19. Aikawa M, Rabkin E, Okada Y, Voglic SJ, Clinton SK, Brinckerhoff CE, Sukhova GK, Libby P. Lipid lowering by diet reduces matrix metalloproteinase activity and increases collagen content of rabbit atheroma: a potential mechanism of lesion stabilization. *Circulation.* 1998;97:2433–2444.
20. Jeanpierre E, Le Tourneau T, Six I, Zawadzki C, Van Belle E, Ezekowitz MD, Bordet R, Susen S, Jude B, Corseaux D. Dietary lipid lowering modifies plaque phenotype in rabbit atheroma after angioplasty: a potential role of tissue factor. *Circulation.* 2003;108:1740–1745.
21. Libby P. Current concepts of the pathogenesis of the acute coronary syndromes. *Circulation.* 2001;104:365–372.
22. Ni W, Egashira K, Kitamoto S, Kataoka C, Koyanagi M, Inoue S, Imaizumi K, Akiyama C, Nishida Ki K, Takeshita A. New Anti-Monocyte Chemoattractant Protein-1 Gene Therapy Attenuates Atherosclerosis in Apolipoprotein E-Knockout Mice. *Circulation.* 2001;103: 2096–2101.
23. Inoue S, Egashira K, Ni W, Kitamoto S, Usui M, Otani K, Ishibashi M, Hiasa K, Nishida K, Takeshita A. Anti-monocyte chemoattractant protein-1 gene therapy limits progression and destabilization of established atherosclerosis in apolipoprotein E-knockout mice. *Circulation.* 2002;106:2700–2706.

Essential Role of Vascular Endothelial Growth Factor in Angiotensin II–Induced Vascular Inflammation and Remodeling

Qingwei Zhao, Minako Ishibashi, Ken-ichi Hiasa, Chunyan Tan, Akira Takeshita, Kensuke Egashira

Abstract—Angiotensin II (Ang II) upregulates vascular endothelial growth factor (VEGF) and activates vascular inflammation. However, the decisive role of VEGF in Ang II–induced vascular inflammation and remodeling has not been addressed. Ang II infusion to wild-type mice increased local expression of VEGF and its receptors in cells of aortic wall and plasma VEGF, and caused aortic inflammation (monocyte infiltration) and remodeling (wall thickening and fibrosis). Hypoxia-inducible factor-1α colocalized with VEGF-positive cell types. Blockade of VEGF by the soluble VEGF receptor 1 (sFlt-1) gene transfer attenuated the Ang II–induced inflammation and remodeling. The sFlt-1 gene transfer also inhibited the increased expression of VEGF and inflammatory factors such as monocyte chemoattractant protein-1. In contrast, sFlt-1 gene transfer did not affect Ang II–induced arterial hypertension and cardiac hypertrophy. VEGF is an essential mediator in Ang II–induced vascular inflammation and structural changes through its proinflammatory actions. (*Hypertension.* **2004;44:264-270.**)

Key Words: growth substances ■ arteriosclerosis ■ remodeling ■ angiotensin II ■ endothelial growth factors

Activation of the renin-angiotensin system as a result of impaired endothelial function plays an important role in the initiation and progression of arteriosclerosis/atherosclerosis through multiple mechanisms.[1–3] We have shown that chronic inhibition of nitric oxide synthesis upregulates angiotensin II (Ang II) production and expression of Ang II type-1 (AT_1) receptor, resulting in vascular inflammation and arteriosclerosis in a rat model.[1,4–7] Ang II augments production of inflammatory cytokines and chemokines by arterial wall cells and monocytes.[8–10] Furthermore, emerging evidence suggests that Ang II is implicated in the process of angiogenesis.[11] Ang II is shown to upregulate vascular endothelial growth factor (VEGF) and promote tumor-associated, VEGF-induced, ischemia-induced angiogenesis in vitro and in vivo.[12–14] There is no report, however, that addressed the role of VEGF in Ang II–induced vascular inflammation and structural changes under in vivo conditions.

VEGF is one of the most potent angiogenic factors known to date and is thought to function as an endogenous regulator of endothelial integrity.[15–18] Previous animals studies have reported that local delivery of VEGF after endothelial injury promotes endothelial regeneration, accelerates the recovery of endothelium-dependent relaxation, and reduces neointimal formation.[18] However, there is still a considerable debate over the vasculoprotective versus pro-inflammatory/arteriosclerotic effects of VEGF.[18] There is emerging evidence that VEGF induces migration and activation of monocytes through induction of adhesion molecules or chemokines such as monocyte chemoattractant protein-1 (MCP-1),[19,20] and that VEGF enhances neointimal formation by stimulating intraplaque angiogenesis[21–23] or by increasing inflammation.[24] Therefore, vasculoprotective versus proinflammatory/arteriosclerotic actions of VEGF remains to be inconclusive.

Accordingly, we aimed to determine the decisive role of VEGF in Ang II–induced vascular remodeling (medial thickening and hypertrophy) in vivo. To determine the role of VEGF in vivo, we used a soluble form of the VEGF receptor-1 (sFlt-1) that blocks VEGF activity by directly sequestering VEGF and by functioning as a dominant-negative inhibitor against VEGF.[25,26] We and other investigators have demonstrated that intramuscular transfection of sFlt-1 gene effectively blocks VEGF, and thus quenches activity of VEGF in vivo.[27,28] We report here that sFlt-1 gene transfer attenuated Ang II–induced vascular inflammation and remodeling in mice. The present study seems to be the first in vivo evidence for an essential role of VEGF in the pathogenesis of Ang II infusion-induced vascular inflammation and remodeling.

Methods

Expression Vector

The 3.3-kb mouse sFlt-1 gene was obtained from a mouse lung cDNA library[25] and cloned into the BamH1(5′) and Not1(3′) sites of the eukaryotic expression vector plasmid cDNA3 (Invitrogen).

Received April 15, 2004; first decision May 4, 2004; revision accepted May 20, 2004.

From the Department of Cardiovascular Medicine, Graduate School of Medical Sciences, Kyushu University, Fukuoka, Japan.

Correspondence to Kensuke Egashira, MD, PhD, Department of Cardiovascular Medicine, Graduate School of Medical Science, Kyushu University, 3-1-1, Maidashi, Higashi-ku, Fukuoka 812-8582, Japan. E-mail egashira@cardiol.med.kyushu-u.ac.jp

Hypertension is available at http://www.hypertensionaha.org

DOI: 10.1161/01.HYP.0000138688.78906.6b

Experimental Animals

The study protocol was reviewed and approved by the Committee of the Ethics of Animal Experiments, Kyushu University Graduate School of Medical Sciences. A part of this study was performed at the Kyushu University Station for Collaborative Research and the Morphology Core, Kyushu University School of Medicine Sciences.

Treatments

Male C57BL/6J wild-type mice were purchased from Jackson Laboratory (Bar Harbor, Me) and fed with commercial standard chow. Mice at 8 to 10 weeks old were randomly divided into 5 groups: (1) the untreated control group; (2) ones receiving Ang II infusion; (3) Ang II infusion plus sFlt-1 gene plasmid transfer; (4) Ang II infusion plus empty plasmid cDNA3 transfer; or (5) Ang II infusion and Ang II AT_1 receptor blocker (olmesartan at 3.5 mg/kg per day, a gift from Sankyo Pharmaceutical Co, Tokyo, Japan) mixed in chow. For Ang II infusion, the osmotic mini-pump (Alzet) containing Ang II saline solution (discharging 1.9 mg/kg of Ang II per day) was implanted in the peritoneal cavity under anesthesia with ketamine (80 mg/kg IP) and xylazine (10 mg/kg IP). Treatment with olmesartan started 3 days before Ang II administration was begun. For gene transfer, either empty plasmid or sFlt-1 plasmid (150 μg/100 μL phosphate-buffered saline per mouse) was injected into both sides of femoral muscles using a 27-gauge needle 1 day before commitment of Ang II infusion, as we previously described.[27,29,30]

In all experiments, mice were euthanized at the indicated time points of treatments for analysis. Venous blood was collected immediately before the mice were euthanized. The aorta and hearts were isolated and either fixed in 10% buffered formalin or snap-frozen. Systolic blood pressure was measured by the tail-cuff method.

Immunohistochemistry, Histopathology, and Morphometry

Immunohistochemistry and histopathology were performed as described previously.[6,29] Some of formalin-fixed and paraffin-embedded cross-sections of abdominal aorta were routinely stained with hematoxylin-eosin or Masson-trichrome. The other sections were subjected to immunostaining assay using antibodies against mouse VEGF and its receptors, Flt-1 and Flk-1 (Santa Cruz Biotech), macrophages (Mac-3; Serotec Inc, Raleigh, NC), proliferating cell nuclear antigen (DAKO, Denmark), α-smooth muscle cell actin (α-SMA; Boehringer Mannheim, Germany), hypoxia-inducible factor-1α (HIF-1α), CD31 (Santa Cruz Biotech), and von Willebrand factor (Sigma Chemical).

Fluorescein FITC-conjugated or rhodamine-conjugated secondary antibodies (Santa Cruz Biotech) were used for double-staining for localization of cell types expressing VEGF and its 2 receptors, or for coexpression of VEGF and HIF-1α. The degree of arteriosclerosis (the medial thickness and perivascular fibrosis) and left ventricle (LV) hypertrophy (LV-to-body weight ratios) on day 28 were measured as described previously.[4,5,7]

TaqMan Real-Time Reverse Transcriptase–Polymerase Chain Reaction

Transcripts of 1 μg total RNA from thoracic and abdominal aorta were reverse-transcribed and the resultant cDNA was amplified by TaqMan real-time reverse transcriptase–polymerase chain reaction as previously described[30] for the following genes: VEGF, Flt-1, Flk-1, HIF-1α, B-type natriuretic peptide, MCP-1, CCR2 (MCP-1 receptor), inteleukin-1 (IL-1), IL-6, transforming growth factor β-1 (TGF-β1), intercellular adhesion molecule-1, and vascular cell adhesion molecule-1. The sequences of sense primers, antisense primers, and the relevant probes were recorded (online Table I available at http://www.hypertensionaha.org). The probe and primers of GAPDH were obtained from Applied Biosystems.

Plasma VEGF and sFlt-1 Measurements

The commercially available enzyme-linked immunosorbent assay kits (Biosource International, Camarillo, Calif) were used to measure

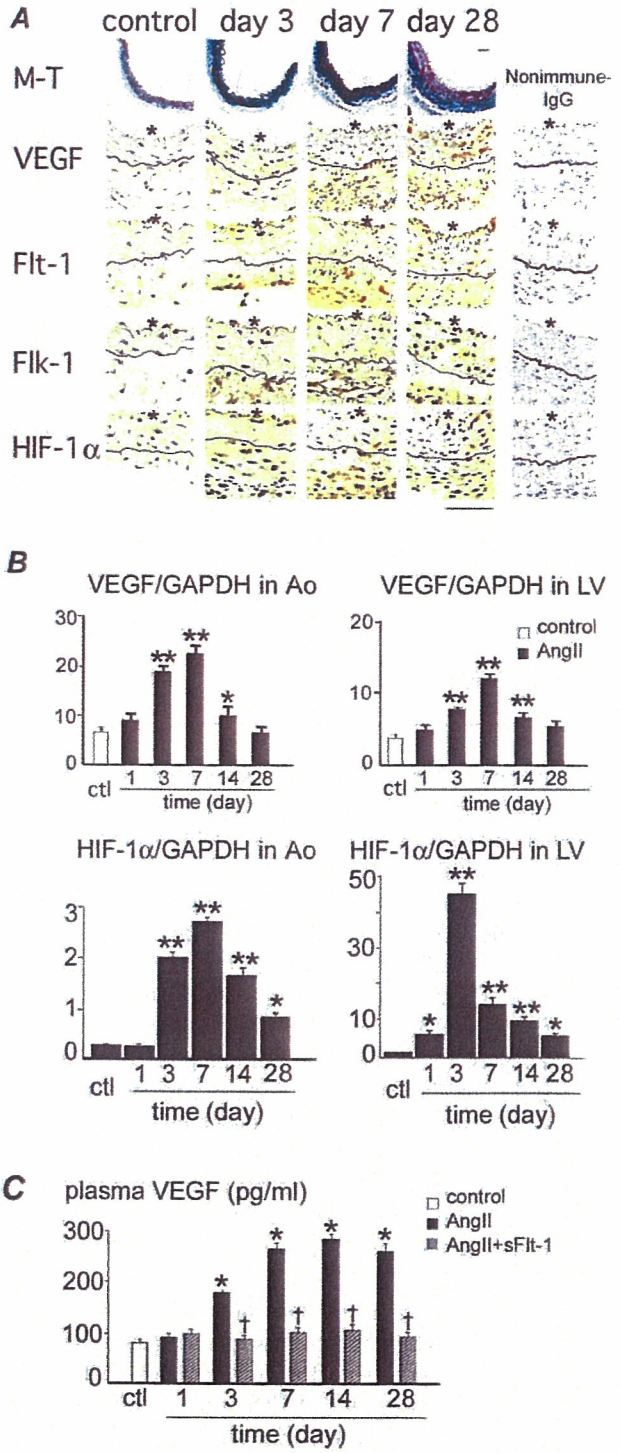

Figure 1. Local and systemic expression of VEGF during Ang II infusion. A, Time courses of Ang II–induced morphological immunohistochemical changes. Cross-sections of abdominal aorta stained with Masson-trichrome (M-T) or with antibodies against VEGF, its 2 receptors Flt-1 and Flk-1, and HIF-1α (positive staining are yellow–brown) are shown. The micrographs at the right of each immunohistochemical staining show negative staining with nonimmune IgG. *Luminal sides of aorta. The black lines indicate external elastic lamina (EEL). Scale bar=50 μm. B, Time courses of mRNA expression of VEGF and HIF-1α in aorta (Ao) and left ventricle (LV). The mRNA value of VEGF or HIF-1α was normalized by GAPDH mRNA in each sample (n=6 to 8). *P<0.05, **P<0.01 vs the untreated control. C, Time course of plasma VEGF level before and after Ang II infusion (n=6 to 8). *P<0.05, **P<0.01 vs the untreated control; †P<0.01 vs Ang II group.

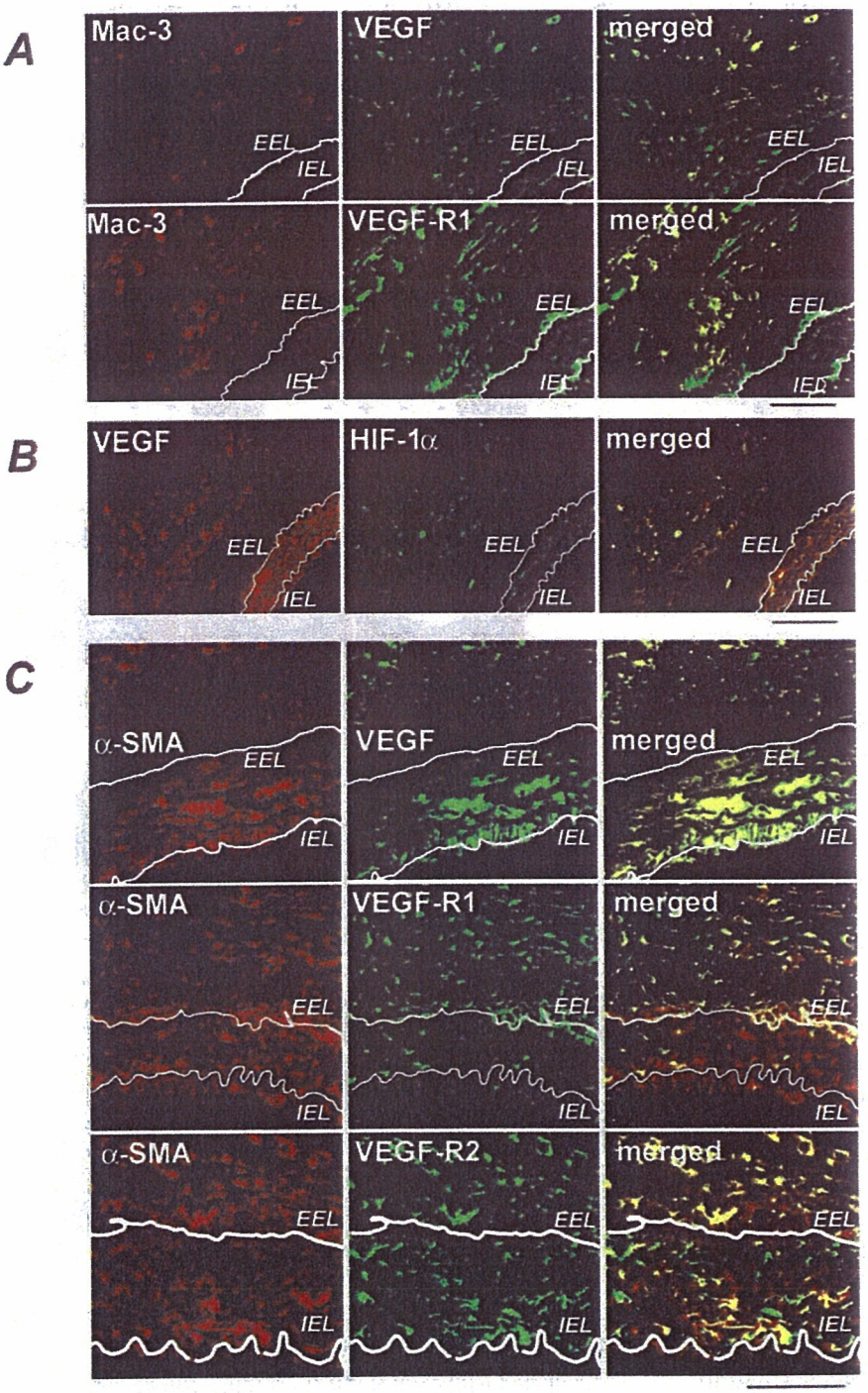

Figure 2. Colocalization of cell types with VEGF and its receptors through immunofluorescent double-staining. A, Some Mac-3–positive macrophages recruited into the adventitia express VEGF or its recepter Flt-1 (VEGF-R1) on day 7. B, VEGF and HIF-1α colocalize in same cell types on day 7. C, α-SM actin–positive cells in medial smooth muscle cells, and adventitial myofibroblast-like cells express VEGF or its receptors on day 28. The white lines indicate EEL or internal elastic lamina (IEL) of aorta. Scale bar=50 μm.

mouse plasma VEGF and soluble Flt-1 according to the manufacturer's instructions.

Statistical Analysis

Data are expressed as the mean±SE. Statistical analysis of differences was compared by analysis of variance. Post hoc analyses were performed using Bonferroni correction for multiple comparison tests. $P<0.05$ was considered to be statistically significant.

Results

Expressions of VEGF, Flt-1, Flk-1, and HIF-1α

Compared with no staining in aortic sections from control mice, intense immunohistochemistrical staining of VEGF, Flt-1, and Flk-1 were seen in aortic sections from mice with Ang II infusion mainly in inflammatory lesions (mononuclear cell infiltration) of the adventitia at an early (days 3 and 7) phase of Ang II infusion (Figure 1A). On day 28, cells in the media also became positive with VEGF and its 2 receptors (Figure 1A). Gene expression of VEGF markedly increased in the aorta and LV. It peaked on day 7 and then spontaneously declined on day 28 (Figure 1B). Because HIF-1α is a transcriptional factor for the control of VEGF expression,[31] immunostaining and mRNA levels of HIF-1α were then examined. HIF-1α expression showed similar temporal and special changes as those of VEGF (Figure 1A and 1B).

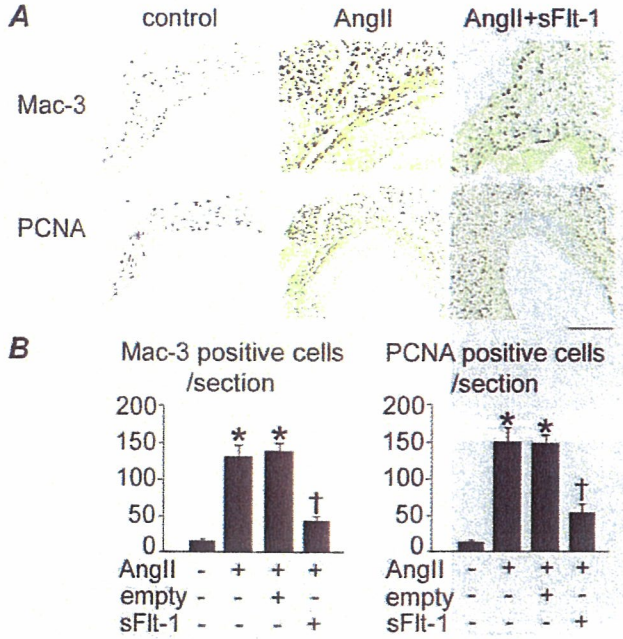

Figure 3. Effects of sFlt-1 gene transfer on inflammatory and proliferative changes. A, Micrographs of aorta with immunostaining against Mac-3 and proliferating cell nuclear antigen before or 7 days after treatments (positive cells in yellow-brown). B, Summary of quantitative analysis in the untreated control, Ang II, Ang II+empty plasmid, and Ang II+sFlt-1 groups (n=6). *P<0.01 vs untreated control, †P<0.01 vs Ang II group. Scale bar=100 μm.

Keeping with rapid upregulation of VEGF in vascular tissues, serial measurements of plasma VEGF showed rapid and persistent increase in the Ang II group (Figure 1C).

To localize VEGF and related signaling, immunofluorescent double staining was performed (Figure 2). On days 3 and 7, Mac-3–positive monocytes recruited to the adventitia and outer layer of the media expressed VEGF and Flt-1 (Figure 2A), but did not express Flk-1 (data not shown). HIF-1α was colocalized in the cell types expressing VEGF (Figure 2B). On day 28, most α-SMA–positive smooth muscle cells in the media expressed VEGF, and some α-SMA–positive cells in the media expressed Flt-1 and Flk-1 (Figure 2C). Some α-SMA–positive myofibroblastic cells in the adventitia expressed VEGF, Flt-1, and Flk-1 (Figure 2C).

No apparent angiogenesis, as detected by von Willebrand factor or CD31 staining, was detected in the aortic wall of the control, Ang II, or Ang II+sFlt-1 groups (data not shown). Furthermore, the endothelial layer of the aorta was preserved in the 3 groups.

Effects of sFlt-1 on Vascular Inflammation and Remodeling

Mac-3–positive monocytes and proliferating cell nuclear antigen-positive proliferating cells were used as the markers of inflammatory and proliferative changes. Infiltration of monocytes and appearance of proliferating cells was markedly increased in the aorta of mice receiving Ang II, particularly in the adventitia on days 3 and 7, which declined spontaneously on day 28. These Ang II–induced inflammatory and proliferative changes in the aorta on day 7 were markedly attenuated in Ang II+sFlt-1 group, but not in the Ang II+empty plasmid group (Figure 3).

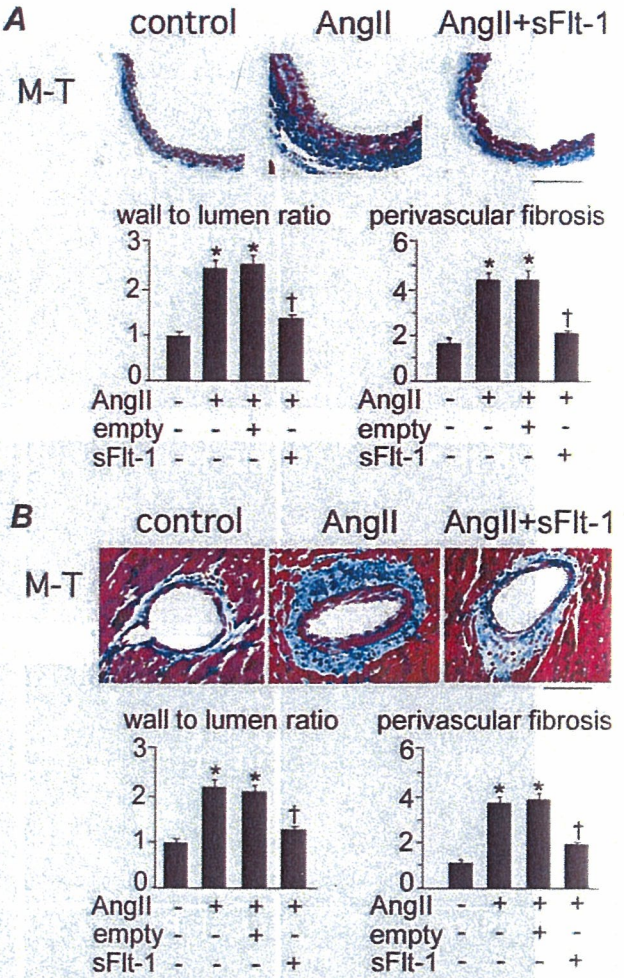

Figure 4. Effects of sFlt-1 gene transfer on Ang II–induced vascular remodeling (medial thickening and perivascular fibrosis). A, Micrographs of cross-sections of abdominal aorta stained with Masson-trichrome on day 28 are shown. Summary of quantitative analysis in untreated control, Ang II, Ang II+empty plasmid, and Ang II+sFl-1 groups are presented (n=6 to 8). Scale bar=100 μm. B, Micrographs of cross-sections of coronary arteries stained with Masson-trichrome on day 28 are shown. Summary of quantitative analysis in untreated control, Ang II, Ang II+empty plasmid, and Ang II+sFl-1 groups are presented (n=6 to 8). *P<0.01 vs untreated control, †P<0.01 versus the Ang II group. Scale bar=50 μm.

Compared with control mice, vascular remodeling (medial wall thickening and perivascular fibrosis) developed in the aorta and coronary arteries from mice received Ang II for 28 days, which was attenuated by sFlt-1 gene transfer but not by empty plasmid transfer (Figure 4A and 4B).

To gain mechanistic insight, mRNA levels of a variety of inflammatory cytokines, chemokines, and chemokine receptors were examined by real-time polymerase chain reaction on day 7 (Figure 5). The sFlt-1 transfection did not affect the increased gene expression of RANTES, MIP-1α, or MIP-2, but prevented or attenuated the increased gene expressions of VEGF, Flt-1 Flk-1, MCP-1, CCR2, IL-1β, IL-6, TGF-β1, vascular cell adhesion molecule-1, intercellular adhesion molecule-1, and HIF-1α (Figure 5). The sFlt-1 transfection

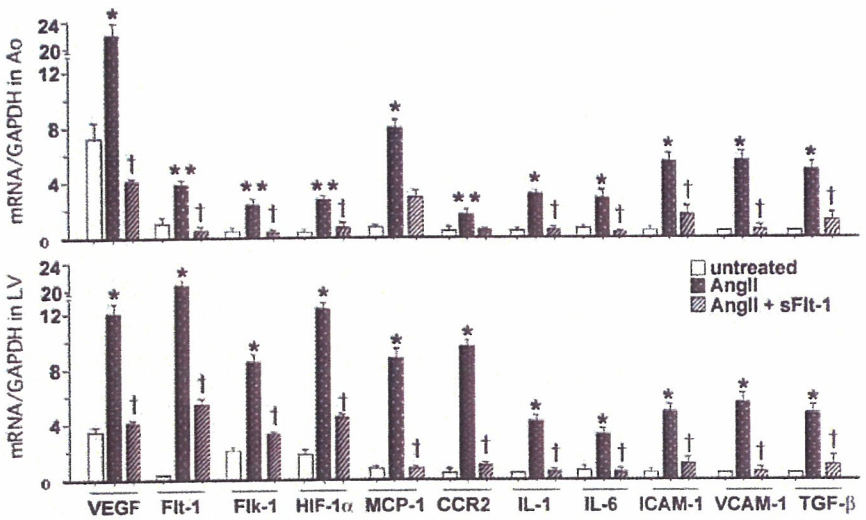

Figure 5. Effects of sFlt-1 gene transfer on Ang II-mediated induction of cytokines and chemokines in aorta and left ventricle on day 7 of Ang II infusion. *$P<0.01$, **$P<0.05$ versus untreated control, †$P<0.01$ vs the Ang II group.

also blunted Ang II–induced increases in plasma VEGF (Figure 1C). Immunohistochemical study revealed that immunoreactive MCP-1, TGF-β1, VEGF, Flt-1, and Flk-1 were increased in Ang II group on day 7 (Figure 6). In contrast, such increased immunostaining was attenuated in aortic sections from the Ang II+sFlt-1 group.

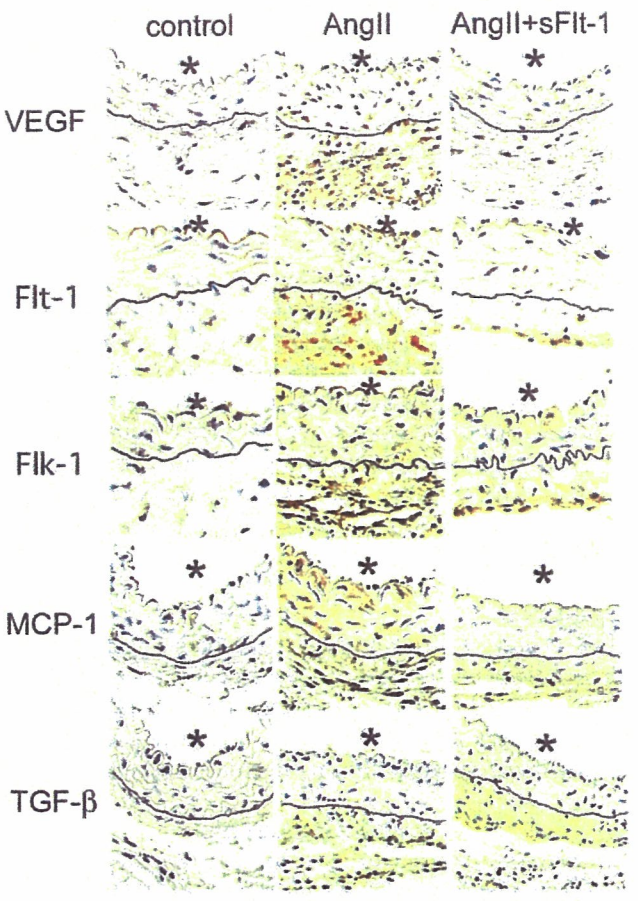

Figure 6. Effects of sFlt-1 gene transfer on immunoreactivities of VEGF, Flt-1, Flk-1, MCP-1, and TGF-β1 on day 7 of Ang II infusion (positive stains in yellow–brown). *Luminal sides of aorta. These immunohistochemical experiments were repeated in 5 sections from different animals, all with representative results. The black lines indicate EEL. Scale bar=50 μm.

Plasma sFlt-1 Concentration

To assess transfection efficacy, plasma sFlt-1 concentration was measured. In control mice, plasma sFlt-1 levels increased on days 3, 7, and 14 (Table 1), indicating that sFlt-1 was released to circulation from the transfected muscle. Similar increase in plasma sFlt-1 levels was noted in mice infused with Ang II.

Systolic Blood Pressure and LV Hypertrophy

Systolic blood pressure was significantly increased in mice receiving Ang II compared with control. There were no significant differences in systolic blood pressure between Ang II and Ang II+sFlt-1 groups (Table 2). To assess the degrees of LV hypertrophy, relative LV weight and B-type natriuretic peptide mRNA levels were determined on day 28 (Table 2). There were no significant differences in Ang II–induced LV hypertrophy or in the increase in B-type natriuretic peptide mRNA levels between Ang II and Ang II+sFlt-1 groups.

Effects of AT_1 Receptor Blocker on Vascular Inflammation and Remodeling

Treatment with AT_1 receptor blocker prevented or markedly attenuated Ang II–induced arterial hypertension, LV hypertrophy (Table 2), and increased immunostaining and gene expression of VEGF, aortic wall inflammation, and arteriosclerotic changes (data not shown). These data suggest that the Ang II–induced increases in VEGF expression and activity were mediated by Ang II AT_1 receptor stimulation.

TABLE 1. Plasma Concentrations of sFlt-1

		Time (day) After sFlt-1 Transfection		
Animal Groups	Baseline	3	7	14
Untreated control	467±37	1037±132*	927±215*	649±83*
Ang II	Not measured	370±23	393±35	383±29
Ang II+sFlt-1	Not measured	1006±22*	1297±24*	730±26*

Mean±SEM (n=6).
*$P<0.01$ vs. baseline in untreated control mice.

TABLE 2. Systolic Blood Pressure, Relative Left Ventricle Weight, and Brain Natriuretic Peptide Gene Expression

Animal Groups	SBP (mm Hg) Day 7	SBP (mm Hg) Day 28	LV/BW Ratio (Day 28)	BNP/GAPDH Ratio (Day 28)
Untreated control	119±3	120±5	4.36±0.12	1.04±0.06
Ang II	176±7*	185±8*	5.12±0.20*	1.91±0.07*
Ang II+ARB	113±6†	117±9†	4.45±0.18†	0.97±0.08†
Ang II+sFlt-1	173±9*	180±12*	5.06±0.11*	2.03±0.15*

SBP indicates systolic blood pressure; LV, left ventricle; BW, body weight; BNP, B-type natriuretic peptide.

Mean±SEM (n=6 to 8).

*$P<0.01$ vs. control; †$P<0.01$ vs. Ang II.

Discussion

Ample evidence suggests that VEGF-mediated signals are essential in Ang II–induced angiogenesis in vivo and endothelial migration/proliferation in vitro.[12–14] The functional importance of VEGF in the mechanism of Ang II–induced vascular inflammation and structural changes, however, has not been addressed. We report here that sFlt-1 gene transfer attenuated the Ang II–induced vascular inflammation and structural changes (medial wall thickening and fibrosis) in mice. Therefore, the present study provides the first in vivo evidence to our knowledge for an essential role of VEGF in the pathogenesis of Ang II infusion-induced inflammation and remodeling.

We examined time-related changes in cell types expressing VEGF and its receptors during Ang II infusion. VEGF was predominately expressed in the lesional monocytes and proliferative myofibroblast, mainly in the adventitial layer at early stages and in smooth muscle cells in the media. This local VEGF expression was associated with rapid and persistent increase in plasma VEGF level. In addition, Flt-1 was increased in lesional monocytes and medial smooth muscle cells at early stages and in medial smooth muscle cells at later stages. No increase in Flk-1 expression was detected in monocytes or myofibroblasts, whereas increased Flk-1 expression was noted in medial smooth muscle cells only at later stages. Our present data show that Ang II-mediated expressions of VEGF and its receptors have a biological effect in inducing vascular inflammation (monocyte infiltration) and proliferation, as well as in causing vascular structural changes. Interestingly, sFlt-1 gene transfer reduced increased local and systemic expression of VEGF, suggesting that sFlt-1 transfection might inhibit VEGF activity at least by trapping VEGF. Because sFlt-1 functions as a nonselective inhibitor of Flt-1 and Flk-1, further studies are needed to elucidate relative role of Flt-1 and Flk-1 in the pathogenesis of Ang II–induced vascular pathobiology.

There are several reports demonstrating that VEGF is a proinflammatory factor.[20,32] In the present study, we extended those observations by showing that sFlt-1 gene transfer attenuated Ang II–induced increase in inflammatory factors in vivo. Regarding the mechanism of VEGF-mediated vascular inflammation, Yamada et al[33] showed that MCP-1 is essential in VEGF-induced angiogenesis and inflammation. Bush et al[34] showed that Ang II–induced vascular inflammation and arteriosclerosis was blunted in mice deficient of MCP-1 receptor. MCP-1 has been shown to be the key chemokine in mediating vascular monocyte-mediated inflammation leading to vascular disease.[35,36] Taken together, it is likely that sFlt-1 gene transfer blocked Ang II–induced vascular structural changes mainly by suppressing inflammation (monocyte recruitment and activation) and subsequent production of growth factors. For example, VEGF-mediated overexpression of TGF-β1 might contribute to Ang II–induced vascular fibrosis. Another interpretation alternative to this conclusion is that increased VEGF and its receptors acted directly on smooth muscle cells, resulting in structural changes such as medial thickening. Several studies have reported that VEGF has direct actions on proliferation/migration of smooth muscle cells,[37,38] which may not be mediated by inflammation (monocyte recruitment). It is possible therefore that some of the mechanism by which sFlt-1 gene transfer inhibited vascular structural changes might not be caused by inflammation.

Regarding the mechanism of Ang II–induced expression of VEGF, we examined HIF-1α expression because HIF-1α plays a major role in the control of VEGF expression. Richard et al[31] reported that Ang II induces VEGF production through HIF-1α in vascular smooth muscle cells in vitro. In the present study, we showed that Ang II infusion increased local HIF-1α expression in vascular wall cells that colocalized in VEGF-expressing cells types, suggesting that increased transcription of HIF-1α is involved in Ang II–induced expression of VEGF.

It is noteworthy that sFlt-1 gene transfer did not affect Ang II–induced arterial hypertension or indices of left ventricular hypertrophy. Arterial blood pressure was, however, measured by the tail-cuff method, a method that cannot provide reliable measure of the pressure changes associated with Ang II infusion. It is reported that arterial hypertension contributes to Ang II–induced vascular remodeling.[39] Furthermore, the dose of Ang II used in the present study was high, which is above the range of physiological condition. Nevertheless, our present observation suggests that VEGF may not be involved in the mechanism of Ang II–induced hypertension or cardiac hypertrophy.

Perspectives

VEGF is likely to be an essential mediator in Ang II–induced vascular inflammation and remodeling but is not involved in Ang II–induced cardiac hypertrophy. Our present data support the notion that VEGF acts as a proinflammatory and proarteriosclerotic factor in Ang II–induced hypertension.

Acknowledgments

This study was supported by grants-in-aid for Scientific Research (14657172, 14207036) from the Ministry of Education, Culture, Sports, Science, and Technology, Tokyo, Japan, by Health Science Research Grants (Comprehensive Research on Aging and Health, and Research on Translational Research) from the Ministry of Health Labor and Welfare, Tokyo, Japan, and by the Program for Promotion of Fundamental Studies in Health Sciences of the Organization for Pharmaceutical Safety and Research, Tokyo, Japan.

References

1. Egashira K. Clinical importance of endothelial function in arteriosclerosis and ischemic heart disease. *Circ J.* 2002;66:529–533.
2. Libby P. Current concepts of the pathogenesis of the acute coronary syndromes. *Circulation.* 2001;104:365–372.
3. Dzau VJ. Theodore Cooper Lecture: Tissue angiotensin and pathobiology of vascular disease: a unifying hypothesis. *Hypertension.* 2001;37: 1047–1052.
4. Takemoto M, Egashira K, Usui M, Numaguchi K, Tomita H, Tsutsui H, Shimokawa H, Sueishi K, Takeshita A. Important role of tissue angiotensin-converting enzyme activity in the pathogenesis of coronary vascular and myocardial structural changes induced by long-term blockade of nitric oxide synthesis in rats. *J Clin Invest.* 1997;99:278–287.
5. Usui M, Egashira K, Tomita H, Koyanagi M, Katoh M, Shimokawa H, Takeya M, Yoshimura T, Matsushima K, Takeshita A. Important role of local angiotensin II activity mediated via type 1 receptor in the pathogenesis of cardiovascular inflammatory changes induced by chronic blockade of nitric oxide synthesis in rats. *Circulation.* 2000;101:305–310.
6. Kitamoto S, Egashira K, Kataoka C, Koyanagi M, Katoh M, Shimokawa H, Morishita R, Kaneda Y, Sueishi K, Takeshita A. Increased activity of nuclear factor-kappaB participates in cardiovascular remodeling induced by chronic inhibition of nitric oxide synthesis in rats. *Circulation.* 2000; 102:806–812.
7. Koyanagi M, Egashira K, Kitamoto S, Ni W, Shimokawa H, Takeya M, Yoshimura T, Takeshita A. Role of monocyte chemoattractant protein-1 in cardiovascular remodeling induced by chronic blockade of nitric oxide synthesis. *Circulation.* 2000;102:2243–2248.
8. Hahn AW, Jonas U, Buhler FR, Resink TJ. Activation of human peripheral monocytes by angiotensin II. *FEBS Lett.* 1994;347:178–180.
9. Hernandez-Presa M, Bustos C, Ortego M, Tunon J, Renedo G, Ruiz-Ortega M, Egido J. Angiotensin-converting enzyme inhibition prevents arterial nuclear factor-kappa B activation, monocyte chemoattractant protein-1 expression, and macrophage infiltration in a rabbit model of early accelerated atherosclerosis. *Circulation.* 1997;95:1532–1541.
10. Kim S, Izumi Y, Yano M, Hamaguchi A, Miura K, Yamanaka S, Miyazaki H, Iwao H. Angiotensin blockade inhibits activation of mitogen-activated protein kinases in rat balloon-injured artery. *Circulation.* 1998;97:1731–1737.
11. Tamarat R, Silvestre JS, Durie M, Levy BI. Angiotensin II angiogenic effect in vivo involves vascular endothelial growth factor- and inflammation-related pathways. *Lab Invest.* 2002;82:747–756.
12. Otani A, Takagi H, Suzuma K, Honda Y. Angiotensin II potentiates vascular endothelial growth factor-induced angiogenic activity in retinal microcapillary endothelial cells. *Circ Res.* 1998;82:619–628.
13. Tamarat R, Silvestre JS, Kubis N, Benessiano J, Duriez M, deGasparo M, Henrion D, Levy BI. Endothelial nitric oxide synthase lies downstream from angiotensin II-induced angiogenesis in ischemic hindlimb. *Hypertension.* 2002;39:830–835.
14. Egami K, Murohara T, Shimada T, Sasaki K, Shintani S, Sugaya T, Ishii M, Akagi T, Ikeda H, Matsuishi T, Imaizumi T. Role of host angiotensin II type 1 receptor in tumor angiogenesis and growth. *J Clin Invest.* 2003;112:67–75.
15. Folkman J. Angiogenesis in cancer, vascular, rheumatoid and other disease. *Nat Med.* 1995;1:27–31.
16. Carmeliet P. Mechanisms of angiogenesis and arteriogenesis. *Nat Med.* 2000;6:389–395.
17. Ferrara N. Role of vascular endothelial growth factor in the regulation of angiogenesis. *Kidney Int.* 1999;56:794–814.
18. Baumgartner I, Isner JM. Somatic gene therapy in the cardiovascular system. *Annu Rev Physiol.* 2001;63:427–450.
19. Barleon B, Sozzani S, Zhou D, Weich HA, Mantovani A, Marme D. Migration of human monocytes in response to vascular endothelial growth factor (VEGF) is mediated via the VEGF receptor flt-1. *Blood.* 1996;87:3336–3343.
20. Marumo T, Schini-Kerth VB, Busse R. Vascular endothelial growth factor activates nuclear factor-kappaB and induces monocyte chemoattractant protein-1 in bovine retinal endothelial cells. *Diabetes.* 1999;48: 1131–1137.
21. Yonemitsu Y, Kaneda Y, Morishita R, Nakagawa K, Nakashima Y, Sueishi K. Characterization of in vivo gene transfer into the arterial wall mediated by the Sendai virus (hemagglutinating virus of Japan) liposomes: an effective tool for the in vivo study of arterial diseases. *Lab Invest.* 1996;75:313–323.
22. Moulton KS, Heller E, Konerding MA, Flynn E, Palinski W, Folkman J. Angiogenesis inhibitors endostatin or TNP-470 reduce intimal neovascularization and plaque growth in apolipoprotein E-deficient mice. *Circulation.* 1999;99:1726–1732.
23. Luttun A, Tjwa M, Moons L, Wu Y, Angelillo-Scherrer A, Liao F, Nagy JA, Hooper A, Priller J, De Klerck B, Compernolle V, Daci E, Bohlen P, Dewerchin M, Herbert JM, Fava R, Matthys P, Carmeliet G, Collen D, Dvorak HF, Hicklin DJ, Carmeliet P. Revascularization of ischemic tissues by PlGF treatment, and inhibition of tumor angiogenesis, arthritis and atherosclerosis by anti-Flt1. *Nat Med.* 2002;8:831–840.
24. Celletti FL, Waugh JM, Amabile PG, Brendolan A, Hilfiker PR, Dake MD. Vascular endothelial growth factor enhances atherosclerotic plaque progression.[comment]. *Nat Med.* 2001;7:425–429.
25. Kondo K, Hiratsuka S, Subbalakshmi E, Matsushime H, Shibuya M. Genomic organization of the flt-1 gene encoding for vascular endothelial growth factor (VEGF) receptor-1 suggests an intimate evolutionary relationship between the 7-Ig and the 5-Ig tyrosine kinase receptors. *Gene.* 1998;208:297–305.
26. Kendall RL, Wang G, Thomas KA. Identification of a natural soluble form of the vascular endothelial growth factor receptor, FLT-1, and its heterodimerization with KDR. *Biochem Biophys Res Commun.* 1996;226: 324–328.
27. Egashira K, Zhao Q, Kataoka C, Ohtani K, Usui M, Charo IF, Nishida K, Inoue S, Katoh M, Ichiki T, Takeshita A. Importance of monocyte chemoattractant protein-1 pathway in neointimal hyperplasia after periarterial injury in mice and monkeys. *Circ Res.* 2002;90:1167–1172.
28. Goldman CK, Kendall RL, Cabrera G, Soroceanu L, Heike Y, Gillespie GY, Siegal GP, Mao X, Bett AJ, Huckle WR, Thomas KA, Curiel DT. Paracrine expression of a native soluble vascular endothelial growth factor receptor inhibits tumor growth, metastasis, and mortality rate. *Proc Natl Acad Sci U S A.* 1998;95:8795–8800.
29. Zhao Q, Egashira K, Inoue S, Usui M, Kitamoto S, Ni W, Ishibashi M, Hiasa Ki K, Ichiki T, Shibuya M, Takeshita A. Vascular endothelial growth factor is necessary in the development of arteriosclerosis by recruiting/activating monocytes in a rat model of long-term inhibition of nitric oxide synthesis. *Circulation.* 2002;105:1110–1115.
30. Usui M, Egashira K, Ohtani K, Kataoka C, Ishibashi M, Hiasa K, Katoh M, Zhao Q, Kitamoto S, Takeshita A. Anti-monocyte chemoattractant protein-1 gene therapy inhibits restenotic changes (neointimal hyperplasia) after balloon injury in rats and monkeys. *FASEB J.* 2002;16: 1838–1840.
31. Richard DE, Berra E, Pouyssegur J. Nonhypoxic pathway mediates the induction of hypoxia-inducible factor 1alpha in vascular smooth muscle cells. *J Biol Chem.* 2000;275:26765–26771.
32. Kim I, Moon SO, Kim SH, Kim HJ, Koh YS, Koh GY. Vascular endothelial growth factor expression of intercellular adhesion molecule 1 (ICAM-1), vascular cell adhesion molecule 1 (VCAM-1), and E- selectin through nuclear factor-kappa B activation in endothelial cells. *J Biol Chem.* 2001;276:7614–7620.
33. Yamada M, Kim S, Egashira K, Takeya M, Ikeda T, Mimura O, Iwao H. Molecular Mechanism and Role of Endothelial Monocyte Chemoattractant Protein-1 Induction by Vascular Endothelial Growth Factor. *Arterioscler Thromb Vasc Biol.* 2003;1:23:1996–2001.
34. Bush E, Maeda N, Kuziel WA, Dawson TC, Wilcox JN, DeLeon H, Taylor WR. CC chemokine receptor 2 is required for macrophage infiltration and vascular hypertrophy in angiotensin II-induced hypertension. *Hypertension.* 2000;36:360–363.
35. Egashira K. Molecular mechanisms mediating inflammation in vascular disease: special reference to monocyte chemoattractant protein-1. *Hypertension.* 2003;41:834–841.
36. Gerard C, Rollins BJ. Chemokines and disease. *Nature Immunology.* 2001;2:108–115.
37. Wang H, Keiser JA. Vascular endothelial growth factor upregulates the expression of matrix metalloproteinases in vascular smooth muscle cells: role of flt-1. *Circ Res.* 1998;83:832–840.
38. Ishida A, Murray J, Saito Y, Kanthou C, Benzakour O, Shibuya M, Wijelath ES. Expression of vascular endothelial growth factor receptors in smooth muscle cells. *J Cell Physiol.* 2001;188:359–368.
39. Kurtz TW. False claims of blood pressure-independent protection by blockade of the renin angiotensin aldosterone system? *Hypertension.* 2003;41:193–196.

Rapid Communication

Bone Marrow–Derived Monocyte Chemoattractant Protein-1 Receptor CCR2 Is Critical in Angiotensin II–Induced Acceleration of Atherosclerosis and Aneurysm Formation in Hypercholesterolemic Mice

Minako Ishibashi, Kensuke Egashira, Qingwei Zhao, Ken-ichi Hiasa, Kisho Ohtani, Yoshiko Ihara, Israel F. Charo, Shinobu Kura, Teruhisa Tsuzuki, Akira Takeshita, Kenji Sunagawa

Abstract—Angiotensin II (Ang II) is implicated in atherogenesis by activating inflammatory responses in arterial wall cells. Ang II accelerates the atherosclerotic process in hyperlipidemic apoE−/− mice by recruiting and activating monocytes. Monocyte chemoattractant protein-1 (MCP-1) controls monocyte-mediated inflammation through its receptor, CCR2. The roles of leukocyte-derived CCR2 in the Ang II-induced acceleration of the atherosclerotic process, however, are not known. We hypothesized that deficiency of leukocyte-derived CCR2 suppresses Ang II-induced atherosclerosis.

Methods and Results—A bone marrow transplantation technique (BMT) was used to develop apoE−/− mice with and without deficiency of CCR2 in leukocytes (BMT-apoE−/−CCR2+/+ and BMT-apoE−/−CCR2−/− mice). Compared with BMT-apoE−/−CCR2+/+ mice, Ang II-induced increases in atherosclerosis plaque size and abdominal aortic aneurysm formation were suppressed in BMT-apoE−/−CCR2−/− mice. This suppression was associated with a marked decrease in monocyte-mediated inflammation and inflammatory cytokine expression.

Conclusion—Leukocyte-derived CCR2 is critical in Ang II-induced atherosclerosis and abdominal aneurysm formation. The present data suggest that vascular inflammation mediated by CCR2 in leukocytes is a reasonable target of therapy for treatment of atherosclerosis. (*Arterioscler Thromb Vasc Biol.* 2003;24:e174-e178.)

Key Words: atherosclerosis ■ angiotensin II ■ inflammation ■ leukocytes

Chronic inflammatory processes have an important role in atherosclerotic plaque progression, destabilization, and subsequent rupture/thrombosis, resulting in acute coronary syndrome.[1,2] Therefore, identification of the critical inflammatory pathway involved in atherosclerotic plaque progression and destabilization might aid in the development of novel therapeutic strategies to reduce atherothrombotic events.

The renin-angiotensin system is now recognized as an important therapeutic target of atherosclerotic vascular disease.[3,4] Angiotensin II (Ang II) induces the production of reactive oxidative species and stimulates the expression of adhesion molecules (vascular cell adhesion molecule-1) and chemokines (monocyte chemoattractant protein-1 [MCP-1]).[3–5] Infusion of Ang II into hypercholesterolemic mice dramatically accelerates the atherosclerotic process, leading to the development of extensive atherosclerotic plaque formation and abdominal aortic aneurysm (AAA).[6,7] The Ang II-mediated acceleration of atherogenesis is characterized by the recruitment and activation of monocytes/macrophages and the degradation of elastin and collagen layers, suggesting that Ang II changes the lesion composition into a more destabilized phenotype. MCP-1 is a C-C chemokine that controls monocyte recruitment to the site of inflammation through its receptor, C-C chemokine receptor (CCR) 2.[8–10] We recently demonstrated that blockade of the MCP-1 pathway by transfection of mutant MCP-1 gene limits Ang II-induced progression and destabilization of atherosclerotic

Original received May 17, 2004; final version accepted August 6, 2004.

From the Department of Cardiovascular Medicine (M.I., K.E., Q.Z., K.H., K.O., Y.I., A.T., K.S.) and the Department of Medical Biophysics and Radiation Biology (S.K., T.T.), Graduate School of Medical Sciences, Kyushu University, Fukuoka, Japan; and the Gladstone Institute of Cardiovascular Disease (I.F.C.), San Francisco, Calif.

Consulting Editor for this article was Alan M. Fogelman, MD, Professor of Medicine and Executive Chair, Departments of Medicine and Cardiology, UCLA School of Medicine, Los Angeles, CA.

Correspondence to Dr Kensuke Egashira, Department of Cardiovascular Medicine, Graduate School of Medical Sciences, Kyushu University, 3-1-1, Maidashi, Higashi-ku, Fukuoka 812-8582, Japan. E-mail egashira@cardiol.med.kyushu-u.ac.jp

Arterioscler Thromb Vasc Biol. is available at http://www.atvbaha.org DOI: 10.1161/01.ATV.0000143384.69170.2d

lesions in hyperlipidemic apoE−/− mice.[11] We and others also demonstrated that blockade or abrogation of MCP-1 or CCR2 attenuates hyperlipidemia-induced atherosclerosis in mice,[12–15] and that CCR2-deficient (CCR2−/−) mice display reduced neointimal formation after arterial injury.[16] Overall, these studies provide ample evidence for a decisive role of MCP-1/CCR2 in atherosclerosis formation, progression, and destabilization.

The role of MCP-1 and/or CCR2 in atherogenesis might be more complex. Ang II is thought to accelerate atherogenesis by stimulating MCP-1 expression and function in multiple cell types in atherosclerotic lesions such as endothelial cells, smooth muscle cells, and leukocytes. Because CCR2 is present in these cell types, activation of the MCP-1–CCR2 pathway mediates recruitment and activation of monocytes,[17] endothelial migration and angiogenesis,[18,19] and migration/proliferation of vascular smooth muscle cells.[20] It is impossible, however, to dissect the relative pathobiologic role of leukocytes versus nonleukocyte cells in the arterial wall using the systemic absence or blockade of MCP-1/CCR2. The aim of this study was to address the role of CCR2 on leukocytes in Ang II-mediated acceleration of the atherosclerotic process. We used bone marrow cell transplantation (BMT) techniques to create a murine model with a leukocyte-derived CCR2 deficiency and demonstrated the essential role of leukocyte-derived CCR2 in Ang II-induced acceleration of atherosclerotic processes.

Methods

Experimental Animals

Male apoE knockout mice were purchased from Jackson Laboratory (Bar Harbor, Me). apoE−/− CCR2−/− and apoE−/− CCR2+/+ mice with the same genetic background (C57BL/6J and 129/svjae hybrids) were supplied by Dr Charo.[12]

Experimental Protocol

The study protocol was reviewed and approved by the Committee on the Ethics of Animal Experiments, Kyushu University Graduate School of Medical Sciences. A part of this study was performed at the Kyushu University Station for Collaborative Research and the Morphology Core Unit, Kyushu University Faculty of Medical Sciences.

To determine the specific role of CCR2 on leukocytes, we used the BMT technique to create mice with and without a leukocyte-selective CCR2 deficiency. At 8 weeks of age, BMT was performed as described previously.[21] Bone marrow cells were harvested from femurs and tibias of either test (apoE−/−CCR2−/−) or control (apoE−/−CCR2+/+) donor mice. The recipient apoE−/−CCR2+/+ mice received 1×10^7 bone marrow cells (0.3 mL) 4 hours after whole body irradiation with 7 Gy of X-rays (200-KVp, 20-mA, 0.3-mm Cu filter) at 1 Gy/min. These 2 groups of mice are referred to as BMT-apoE−/−CCR2−/− and BMT-apoE−/−CCR2+/+, respectively. At 14 weeks of age, BMT-apoE−/−CCR2−/− and BMT-apoE−/−CCR2+/+ mice were infused with Ang II (1.9 mg/kg per day) or phosphate-buffered saline via osmotic mini-pump (Alzet, Cupertino, Calif).[21]

In all experiments, mice were euthanized on day 7 or 28 of treatment for morphometric, immunohistochemical, and biochemical analysis. Peripheral arterial blood was collected immediately before the mice were euthanized. The aortas were isolated and either fixed in 10% buffered formalin for histological and immunohistochemical analysis or snap-frozen in liquid nitrogen (LN_2) and stored at −80°C for biochemical analysis. Systolic blood pressure was measured by the tail-cuff method before and 28 days after treatment.

Histology and Immunohistochemistry

To quantify the extent of the atherosclerotic lesions, the aortic arch and the thoracic aorta was opened longitudinally, stained with oil red O, and pinned out on a black wax surface. The percentage of the plaque area stained by oil red O to the total luminal surface area was determined.

To further quantify the atherosclerotic lesions in the aortic root, serial cryostat sections (6 μm) of the aortic root were prepared as described.[14] In brief, atherosclerotic lesions in the aortic root were examined at 5 locations, each separated by 120 μm, 4 to 5 serial sections were prepared from each location. Some of these sections were stained with Elastica van Gieson and oil red O (for lipid staining). Elastica van Gieson staining was used to delineate the internal elastic lamina for determination of the intimal area. The lipid composition of the lesion was determined by calculating the percent of the oil red O positive area to the total cross-sectional vessel wall area. The remaining sections were used for immunohistochemical analysis. Air-dried cryostat sections were fixed in acetone and stained with the respective antibody: antimouse macrophage antibodies (Mac-3; Serotec Inc, Raleigh, NC) and antihuman MCP-1 antibodies (Santa Cruz Biotechnology Inc, Santa Cruz, Calif). The sections were then counterstained with hematoxylin. Respective nonimmune IgGs (Dako) were used as negative controls. Similarly, the number of macrophage accumulated into the aortic root lesion was estimated.

A single observer blinded to the experiment protocol performed quantitative analysis of atherosclerotic lesions. All images were captured with a Nikon microscope equipped with a video camera and analyzed using Adobe Photoshop 6.0 and National Institutes of Health Image Software. In each case, the average value for 4 to 5 locations or sections for each animal was used for analysis.

Real-Time Reverse-Transcription Polymerase Chain Reaction Analysis

Real-time polymerase chain reaction amplification was performed with the mouse cDNA using the ABI PRISM 7000 Sequence Detection System (Applied Biosystems).[21] The respective polymerase chain reaction primers and TaqMan probes were designed from GenBank databases using a software program (Table I, available online at http://atvb/ahajournals.org).

Flow Cytometry Analysis

Flow cytometry analysis was performed as described previously.[21] To determine CCR2 expression in monocytes, antibodies against phycoerythrin-conjugated antimouse monocyte (CD80) (Becton Dickinson Biosciences, San Jose, Calif), goat antimouse CCR2 (Santa Cruz Biotechnology Inc), and fluorescein isothiocyanate-conjugated mouse antigoat IgG (Santa Cruz Biotechnology Inc) were used. To determine CCR2 fluorescence intensity in lymphocytes and neutrophils, leukocytes were also stained using antibodies against phycoerythrin-conjugated antimouse CD11b (Mac-1), cy-chrome–conjugated antimouse T-cell receptor β chain monoclonal antibody (Becton Dickinson Biosciences). In control experiments, fluorescein isothiocyanate-conjugated nonspecific goat IgG was used to measure nonspecific binding. Stained cells were analyzed by fluorescence-activated cell sorter Calibur (Becton Dickinson Biosciences).

Plasma Measurements

Commercially available enzyme-linked immunosorbent assay kits (Biosource International, Camarillo, Calif) were used to measure plasma total cholesterol, triglyceride, low-density lipoprotein cholesterol, and mouse MCP-1 according to the manufacturer's instructions.

Statistical Analysis

Data were expressed as mean±SEM. Statistical analysis of differences was compared by analysis of variance using Bonferroni correction for multiple comparisons. $P<0.05$ was considered statistically significant.

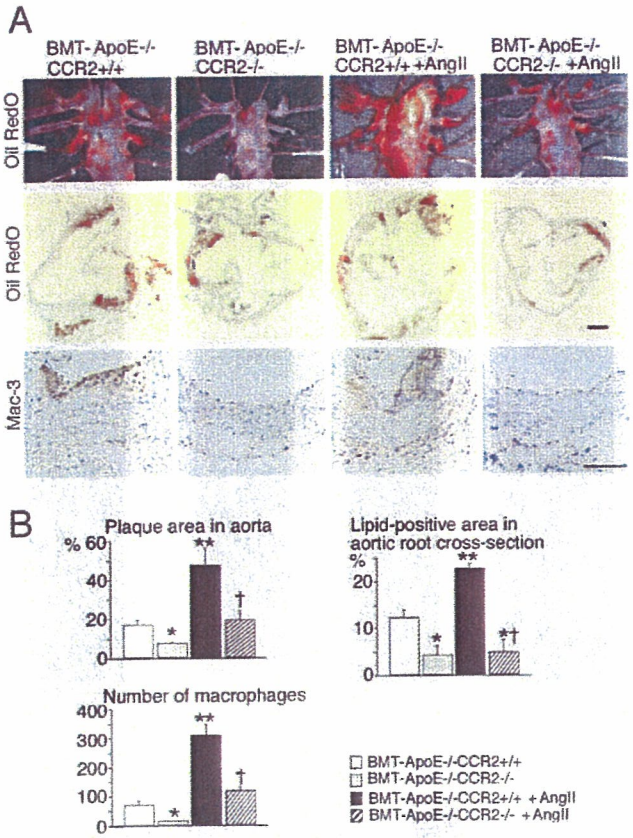

Figure 1. Suppressed Ang II-induced atherosclerotic lesions in BMT-apoE−/− CCR2−/− mice. A, Histopathologic and immunohistochemical pictures of atherosclerotic lesions. From the top to bottom panels, photomicrographs of the intraluminal surface of the aortic arch and thoracic aorta stained with oil red O, those of atherosclerotic lesions in the aortic root stained with oil red O, and those of atherosclerotic lesions in the aortic root immunostained with antimurine macrophage antibody (Mac-3). Bar indicates 100 μm. B, Quantitative comparison of atherosclerotic lesion size (% of oil red O stained area) in BMT-apoE−/−CCR2+/+,BMT-apoE−/−CCR2−/−, BMT-apoE−/−CCR2+/+ + Ang II, and BMT-apoE−/−CCR2−/− + Ang II groups. Data are reported as mean±SEM. N=6 to 8. *P<0.05, **P<0.01 versus BMT-apoE−/−CCR2+/+ group. †P<0.05, ††P<0.01 versus BMT-apoE−/−CCR2+/+ + Ang II group.

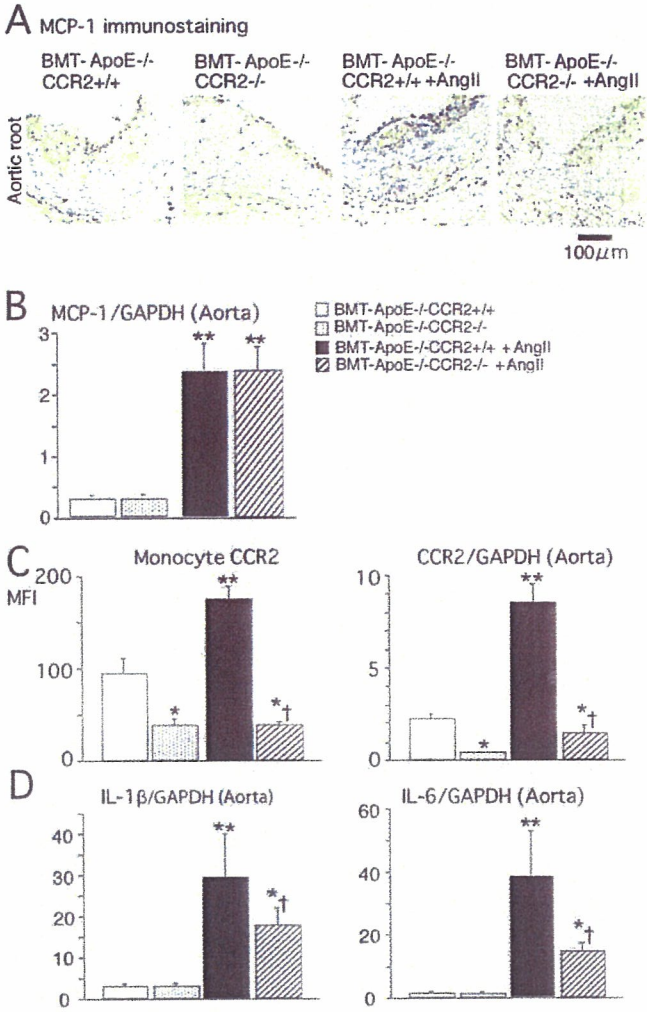

Figure 2. MCP-1, CCR2, and cytokine expression. A, Photomicrographs of cross-sections of the aortic root stained immunohistochemically for MCP-1 on day 28. Bar indicates 100 μm. B, MCP-1 gene expression by real-time reverse-transcription polymerase chain reaction in the aorta on day 7. Data are expressed as the ratio of MCP-1 mRNA to GAPDH mRNA. **P<0.01 versus BMT-apoE−/−CCR2+/+ group (n=6 each). C, CCR2 antigen expression on peripheral blood circulating monocytes by flow cytometry analysis. CCR2 gene expression of the aorta by real-time reverse-transcription polymerase chain reaction on day 7. Data are expressed as the ratio of MCP-1 mRNA to GAPDH mRNA. *P<0.05, **P<0.01 versus BMT-apoE−/−CCR2+/+ group; †P<0.05 versus BMT-apoE−/−CCR2+/+ + Ang II group (n=6 each). D, IL-1β and IL-6 gene expression by real-time reverse-transcription polymerase chain reaction in the aorta on day 7. Data are expressed as the ratio of MCP-1 mRNA to GAPDH mRNA. *P<0.05, **P<0.01 versus BMT-apoE−/−CCR2+/+ group; †P<0.05 versus BMT-apoE−/−CCR2+/+ + Ang II group (n=6 each).

Results

Bone Marrow-Derived CCR2 Is Critical for Ang II-Induced Acceleration of Atherosclerosis

To determine the role of BM-derived CCR2, Ang II was infused in BMT-apoE−/−CCR2+/+ and BMT-apoE−/−CCR2−/− mice. As reported previously,[11] Ang II infusion accelerates atherosclerotic process in BMT-apoE−/−CCR2+/+ mice. In contrast, Ang II-induced acceleration of atherosclerosis was suppressed in BMT-apoE−/−CCR2−/− mice (Figure 1A and 1B). In addition, Ang II-induced aortic inflammatory changes as well as lipid accumulation were markedly attenuated in BMT-apoE−/−CCR2−/− mice (Figure 1A and 1B).

Ang II-induced gene and protein expression of MCP-1 was examined 7 days after Ang II-infusion. Ang II infusion increased MCP-1 mRNA and immunoreactive MCP-1 levels in the aortic root, which were similar between BMT- apoE−/−CCR2+/+ and BMT-apoE−/−CCR2−/− mice (Figure 2A and 2B). Aortic CCR2 gene expression was also suppressed in BMT- apoE−/−CCR2−/− mice infused with and without Ang II (Figure 2C).

Ang II-induced changes in CCR2 antigen on circulating leukocytes were examined by flow cytometric analysis on day 7. Ang II infusion increased CCR2 antigen on monocytes in BMT-apoE−/−CCR2+/+ mice, which was blunted in BMT-apoE−/−C CR2−/− mice (Figure 2C). No CCR2 antigen was detected on lymphocytes or neutrophils in the presence or absence of Ang II infusion (data not shown).

These cytometric data indicate that CCR2 antigen was expressed mainly on circulating monocytes whether Ang II was infused.

In BMT- apoE−/−CCR2+/+ mice, Ang II infusion enhanced gene expression of IL-6 and IL-1β in the aorta on day 7 (Figure 2D). The Ang II-induced increases in IL-6 and IL-1β gene expression were reduced in BMT-apoE−/−CCR2−/− mice.

There were no significant differences in plasma MCP-1 levels between BMT-CCR2+/+ mice infused with or without Ang II on day 28 (Table I). There were no significant differences in Ang II-induced changes in systolic blood pressure or serum lipid levels (Table II, available online at http://atvb.ahajournals.org), suggesting that the observed effects of leukocyte-derived CCR2 deficiency cannot be explained by the effects on plasma lipids or Ang II-induced arterial hypertension. There were no significant differences in plasma MCP-1 levels between untreated BMT-apoE−/−CCR2+/+ and BMT-apoE−/−CCR2−/− mice on day 28 (Table II). In contrast, the plasma MCP-1 level dramatically increased in BMT-apoE−/−CCR2−/− mice infused with Ang II, compared with that in BMT-apoE−/−CCR2+/+ mice infused with Ang II.

Ang II-Induced AAA Formation Is Suppressed in BMT-ApoE−/−CCR2−/− Mice

As reported by others,[6,7] Ang II infusion induced AAA formation associated with the recruitment and activation of monocytes/macrophages into the adventitia and media and the degradation of elastin and collagen layers (Figure 3A). In separate experiments, to determine the effect of BM-derived CCR2 deficiency on Ang II-induced aneurysm formation, we quantified the incidence and measured the diameter of AAA. Mice that displayed 10% increase in abdominal aortic diameter were defined to have AAA. Compared with BMT-apoE−/−CCR2+/+ mice, BMT-apoE−/−CCR2−/− mice showed a significant reduction in the incidence of AAA formation (9 of 10 BMT-apoE−/−CCR2+/+ mice had AAAs versus only 1 of 10 for BMT-apoE−/−CCR2−/− mice; $P<0.01$). Furthermore, the Ang II-induced increase in maximum diameter of the abdominal aorta was not observed in BMT-apoE−/−CCR2−/− mice (Figure 3B).

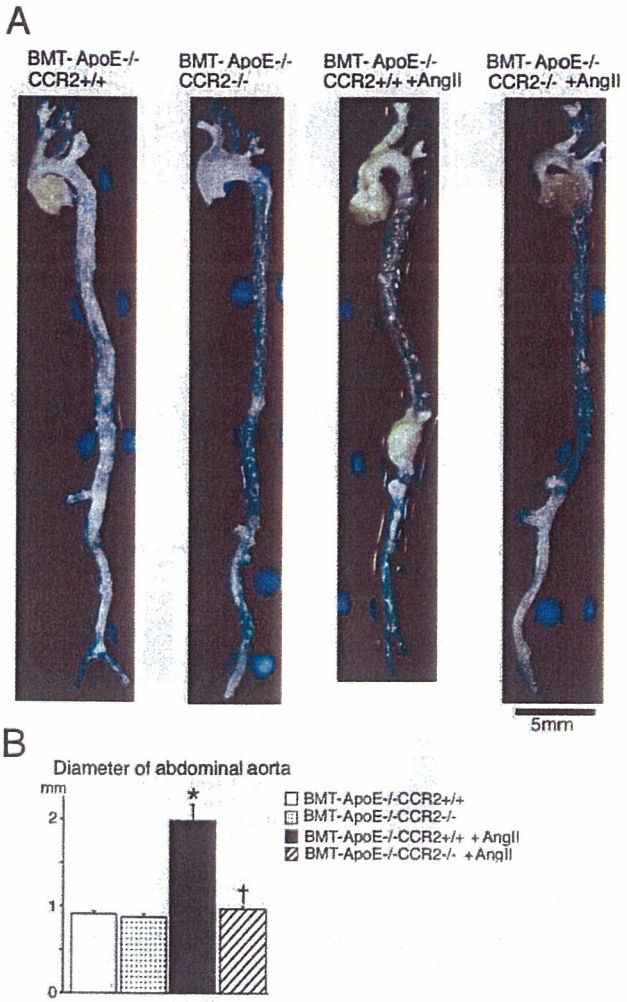

Figure 3. Suppression of Ang II-induced abdominal aortic aneurysm formation in BMT-apoE−/−CCR2−/− mice. A, Photomicrographs of the gross appearance of the ascending aorta to the abdominal aorta. There was significant abdominal aortic aneurysm formation in BMT-apoE−/−CCR2+/+ mice infused with Ang II, whereas there was no aneurysm formation in BMT-apoE−/−CCR2−/− mice. B, Diameters of the abdominal aorta. N=10 each. *$P<0.01$ versus BMT-apoE−/−CCR2+/+ mice with no Ang II infusion. †$P<0.01$ versus BMT-apoE−/−CCR2+/+ mice with Ang II infusion.

Discussion

The important and novel finding of this study was suppressed Ang II-induced acceleration of atherosclerotic process in BMT-apoE−/−CCR2−/− mice. The present study, therefore, represents the first direct evidence for the critical role of CCR2 on leukocytes, especially on monocytes, in Ang II-induced acceleration of atherosclerosis.

BMT from apoE−/−CCR2−/− to apoE−/−CCR2+/+ mice was associated with blunted expression of CCR2 antigen on circulating leukocytes, especially on circulating monocytes. This BMT-apoE−/−CCR2−/− mice displayed suppressed monocyte/macrophage infiltration and lipid accumulation into the atherosclerotic lesions induced by Ang II infusion. To elucidate the mechanism of suppressed Ang II-induced inflammation in BMT-apoE−/−CCR2−/− mice, we examined local and systemic expression of MCP-1. The lack of a detectable difference in Ang II-induced local MCP-1 expression between BMT-apoE−/−CCR2+/+ and BMT-apoE−/−CCR2−/− mice suggests that suppression of Ang II-induced inflammation might result from the lack of CCR2 on monocytes, but not the result of reduced expression of MCP-1. The increase in plasma MCP-1 concentrations in BMT-apoE−/−CCR2+/+ and BMT-apoE−/−CCR2−/− mice infused with Ang II might reflect compensatory local overproduction of MCP-1 in any tissue, including vascular tissues. The present data of attenuated gene expression of inflammatory cytokines in the aorta from BMT-apoE−/−CCR2−/− mice support the notion that activated lesional leukocytes might produce inflammatory and growth-promoting signals, which in turn lead to further acceleration of atherosclerosis. Our present data suggest that anti-inflammation caused by blockade of CCR2-mediated mono-